CHEMISTRY
A EUROPEAN JOURNAL

DOI: 10.1002/chem.201001486

Synthesis and Reactivity of Boron-, Silicon-, and Tin-Bridged *ansa*-Cyclopentadienyl–Cycloheptatrienyl Titanium Complexes (Troticenophanes)

Holger Braunschweig,*[a] Marco Fuß,[a] Swagat K. Mohapatra,[b] Katharina Kraft,[a] Thomas Kupfer,[a] Melanie Lang,[a] Krzysztof Radacki,[a] Constantin G. Daniliuc,[b] Peter G. Jones,[b] and Matthias Tamm*[b]

Abstract: A novel one-pot method was developed for the preparation of [Ti(η^5-C_5H_5)(η^7-C_7H_7)] (troticene, **1**) by reaction of sodium cyclopentadienide (NaCp) with [$TiCl_4(thf)_2$], followed by reduction of the intermediate [(η^5-C_5H_5)$_2TiCl_2$] with magnesium in the presence of cycloheptatriene (C_7H_8). The [*n*]troticenophanes **3** (*n* = 1), **4**, **8**, **10** (*n* = 2), and **11** (*n* = 3) were synthesized by salt elimination reactions between dilithiated troticene, [Ti(η^5-C_5H_4Li)(η^7-C_7H_6Li)]·pmdta (**2**) (pmdta = *N*,*N*′,*N*′,*N*″,*N*″-pentamethyldiethylenetriamine), and the appropriate organoelement dichlorides $Cl_2Sn(Mes)_2$ (Mes = 2,4,6-trimethylphenyl), $Cl_2Sn_2(tBu)_4$, $Cl_2B_2(NMe_2)_2$, $Cl_2Si_2Me_4$, and $(ClSiMe_2)_2CH_2$, respectively. Their structural characterization was carried out by single-crystal X-ray diffraction and multinuclear NMR spectroscopy. The stanna[1]- and stanna[2]troticenophanes **3** and **4** represent the first heteroleptic sandwich complexes bearing Sn atoms in the *ansa* bridge. The reaction of **3** with [$Pt(PEt_3)_3$] resulted in regioselective insertion of the [$Pt(PEt_3)_2$] fragment into the Sn–C_{ipso} bond between the tin atom and the seven-membered ring, which afforded the platinastanna[2]troticenophane **5**. Oxidative addition was also observed upon treatment of **4** with elemental sulfur or selenium, to produce the [3]troticenophanes [Ti(η^5-$C_5H_4SntBu_2$)(η^7-$C_7H_6SntBu_2$)E] (**6**: E = S; **7**: E = Se). The B–B bond of the bora[2]troticenophane **8** was readily cleaved by reaction with [$Pt(PEt_3)_3$] to form the corresponding oxidative addition product [Ti(η^5-$C_5H_4BNMe_2$)(η^7-$C_7H_6BNMe_2$)Pt(PEt_3)$_2$] (**9**). The solid-state structures of compounds **5**, **6**, and **9** were also determined by single-crystal X-ray diffraction.

Keywords: metallocenes · oxidative addition · sandwich complexes · titanium · troticenophanes

Introduction

Since the breakthrough by Osborne et al. in synthesizing a silicon-bridged [1]ferrocenophane in 1975,[1] the structural properties and reactivity patterns of this class of compounds have been the subject of great interest in current research. These molecules provide striking examples of strained structures; a single bridging element is introduced between the two cyclopentadienyl units of the ferrocene framework, which results in ring-tilted structures. Prominent contributions from Manners' group suggested their use as novel precursors for the preparation of high-molecular-weight poly(metallocenes) by facile thermal, anionic, photoinduced, or transition-metal-catalyzed ring-opening polymerization (ROP) reactions. Furthermore, alternative approaches to poly(ferrocenes) have been developed, for example, condensation reactions of unstrained diborylated systems leading to borylene-bridged macromolecules.[2] Since then, the area of strained ferrocenophanes has been expanded significantly; in particular, the nature of the bridging moiety has been varied to include the main-group elements of group 13 (B, Al, Ga),[3] group 14 (Ge, Sn),[4] group 15 (P, As),[4a,5] and group 16 (S, Se)[6] and the early and late transition metals of group 4 (Ti, Zr, Hf)[7] and group 10 (Ni, Pt).[8] In contrast to ferrocene, the related chemistry of non-iron metallocenes such as ruthenocene,[9] cobaltocene,[10] and nickelocene,[11]

[a] Prof. Dr. H. Braunschweig, M. Fuß, K. Kraft, Dr. T. Kupfer, M. Lang, Dr. K. Radacki
Institut für Anorganische Chemie
Julius Maximilians-Universität Würzburg
Am Hubland, 97074 Würzburg (Germany)
Fax: (+49) 931-31-84623
E-mail: h.braunschweig@mail.uni-wuerzburg.de

[b] Dr. S. K. Mohapatra, Dr. C. G. Daniliuc, Prof. Dr. P. G. Jones, Prof. Dr. M. Tamm
Institut für Anorganische und Analytische Chemie
Technische Universität Carolo-Wilhelmina zu Braunschweig
Hagenring 30, 38106 Braunschweig (Germany)
Fax: (+49) 531-391-5387
E-mail: m.tamm@tu-bs.de

has not been extensively developed,[10] and the situation is even worse for homoleptic non-metallocene systems, such as bis(benzene)vanadium,[12,13] bis(benzene)chromium,[12f,13,14] and bis(benzene)molybdenum,[15] even though these sandwich complexes have been known for decades. Recently, the preparation of strained organometallic complexes has been extended to a new class of sandwich compounds of the formula $[M(\eta^5\text{-}C_5H_5)(\eta^7\text{-}C_7H_7)]$ (M = Ti, V, Cr), which resulted in the formation of *ansa*-cyclopentadienyl–cycloheptatrienyl (Cp-Cht) complexes of the type $[M(\eta^5\text{-}C_5H_4)(\eta^7\text{-}C_7H_6)ER_x]$ (M = Ti, V, Cr) (Figure 1).[16–18] Such systems, which are isoelectronic with the corresponding bis(benzene) sandwich complexes, display variable spectroscopic and electronic properties[17,18] and are thus of interest from a theoretical point of view and also with respect to their potential use as organometallic precursors for the preparation of metallopolymers and advanced materials.

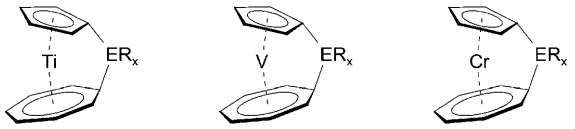

Figure 1. *Ansa* complexes of the type $[M(\eta^5\text{-}C_5H_4)(\eta^7\text{-}C_7H_6)ER_x]$ (M = Ti, V, Cr; E = bridging element). **A**: Tamm et al.; $ER_x = SiMe_2$, $GeMe_2$, $SiMe_2$–$Pt(PEt_3)_2$, $GeMe_2$–$Pt(PEt_3)_2$. **B**: Elschenbroich et al.; $ER_x = SiPh_2$, Si_2Me_4; Tamm et al.; $ER_x = SiMe_2$, $SiMe_2$–$Pt(PEt_3)_2$; Braunschweig et al.; $ER_x = BN(SiMe_3)_2$, $B_2(NMe_2)_2$. **C**: Braunschweig et al.; $ER_x = SiMe_2$, Si(*i*Pr)$_2$, SiMe*i*Pr, $Si(CH_2)_3$, $GeMe_2$, $BN(SiMe_3)_2$, Si_2Me_4, $B_2(NMe_2)_2$, $SiMe_2$–$Pt(PEt_3)_2$. VE = valence electrons.

Although the synthetic protocols for these mixed sandwich complexes $[M(\eta^5\text{-}C_5H_5)(\eta^7\text{-}C_7H_7)]$ (M = group 4–6 metals) were explored a long time ago,[19] their preparation in high yield and sufficient purity still remains challenging, as does their selective functionalization. Recently, the groups of Tamm (M = Ti, Zr, Hf, V),[20,21] Elschenbroich (M = V),[16,22] and Braunschweig (M = V, Cr)[23,24] have provided significant contributions to the chemistry of these transition-metal systems. Elschenbroich reported the syntheses of sila- and disila-bridged trovacenophanes in 2004 by dilithiation of trovacene with an excess of BuLi/tmeda (tmeda = *N*,*N*,*N*′,*N*′-tetramethylethylenediamine) and subsequent treatment with the appropriate dihaloorganosilanes.[16] In the same year, Tamm elaborated the preparation of sila- and germatroticenophanes following the same approach.[20a,c] Subsequently, Braunschweig extended this chemistry by reports of bora-, sila-, and germatrochrocenophanes[24] and boratrovacenophanes.[23] Representative examples are shown in Figure 1. In all cases, selective lithiation of the Cht and Cp rings proved to be the key step for the investigation of such mixed sandwich complexes. In particular, Braunschweig (2007)[24c] and Tamm (2009)[25] provided viable protocols for the selective and high-yield dilithiation of trochrocene and troticene by using *t*BuLi/tmeda and *n*BuLi/pmdta (pmdta = *N*,*N*′,*N*′,*N*″,*N*″-pentamethyldiethylenetriamine), respectively, and also the full spectroscopic and structural characterization of the dilithio species by NMR spectroscopy and X-ray diffraction analysis. It should be noted that this protocol for the preparation of [*n*]metalloarenophanes has been extended to other classes of heteroleptic sandwich systems such as $[Mn(\eta^5\text{-}C_5H_5)(\eta^6\text{-}C_6H_6)]$[26] and $[Co(\eta^4\text{-}C_4Me_4)(\eta^5\text{-}C_5H_5)]$.[27]

With efficient dilithiation protocols at hand, our groups have developed a mutual interest in expanding the range of element-bridged troticenophanes, and our joint efforts are presented herein. We provide full details of the synthesis and structural characterization of stanna-, distanna-, disila-, and dibora-bridged troticenophanes together with a study of their susceptibility towards cleavage of Sn–C, Sn–Sn, and B–B bonds.

Results and Discussion

Synthesis of $[Ti(\eta^5\text{-}C_5H_5)(\eta^7\text{-}C_7H_7)]$ (1): The synthesis of troticene (**1**) is a well-known reaction, first reported by van Oven in 1970. Typically, a mixture of cycloheptatriene (C_7H_8), catalytic amounts of $FeCl_3$, and a reducing agent such as Mg or *i*PrMgCl is treated with $[(\eta^5\text{-}C_5H_5)TiCl_3]$ to afford troticene after workup in variable yields of 33 to 88%, depending on the reaction conditions.[28] Although the reported yields are satisfying, a time-consuming multistep reaction sequence is required. Therefore, we decided to reinvestigate the synthesis of $[Ti(\eta^5\text{-}C_5H_5)(\eta^7\text{-}C_7H_7)]$ (**1**) in order to develop a one-pot reaction procedure. In analogy to the preparation of disubstituted group 4 phosphine complexes of the type $[M(\eta^5\text{-}C_5H_4PR_2)(\eta^7\text{-}C_7H_7)]$ (M = Zr, Hf; R = *i*Pr, Ph),[21a] **1** was prepared by addition of two equivalents of NaCp to a solution of $[TiCl_4(thf)_2]$ in THF, which yielded the intermediate $[(\eta^5\text{-}C_5H_5)_2TiCl_2]$. Subsequent reaction with a mixture of cycloheptatriene and Mg turnings in THF afforded $[Ti(\eta^5\text{-}C_5H_5)(\eta^7\text{-}C_7H_7)]$ (**1**) in acceptable yields of 50% (Scheme 1).

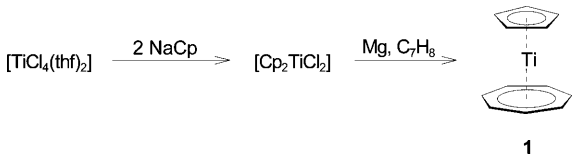

Scheme 1. Synthesis of troticene (**1**).

During the purification of **1** by sublimation, colorless crystals formed, which could be separated mechanically and were identified as $[Mg(\eta^5\text{-}C_5H_5)_2]$·thf by ^{1}H NMR spectroscopy.[29] As expected, the Cp and Cht ring protons of **1** show two distinct singlets at $\delta = 4.91$ and 5.43 ppm integrating to five and seven protons, respectively. These data are in excellent agreement with previous reports.[20a,28a] Furthermore, the ^{13}C NMR spectrum exhibits two resonances at $\delta = 86.40$ (C_7H_7) and 97.04 ppm (C_5H_5).

Syntheses of [*n*]troticenophanes (*n* = 1–3): We have previously reported the synthesis of [1]troticenophanes bearing Si and Ge atoms in bridging positions by salt metathesis reactions between dilithiotroticene and the organoelement dichlorides Cl_2SiMe_2 and Cl_2GeMe_2.[20a,c] These molecules possess strained structures with tilt angles between the planes of the C_5H_4 and C_7H_6 rings of $\alpha = 24.1°$ and 22.9°, respectively; the angles between the E–C_{ipso} bonds and the planes of the five- and seven-membered rings range from $\beta = 28.5°$ to 42.3°. We also established that these species regioselectively insert the $[Pt(PEt_3)_2]$ fragment into the highly strained E–C_{ipso} bonds. The properties of strained organometallic *ansa* complexes could be modified by changing the bridging element E, and thus, given a viable dilithiation protocol, the synthesis of troticenophanes by inclusion of other bridging elements would be of considerable interest. In addition, [2]metalloarenophanes have proved to be excellent starting materials for the functionalization of organic substrates; for instance, bora[2]metalloarenophanes (M = Cr and V) have been used as diborane(4) sources in Pt^0-catalyzed diboration reactions of alkynes and azobenzene.[12b,30] Under drastic conditions, this method has been extended to the disilylation of propyne in the presence of $[Pd(PPh_3)]_4$.[14a]

Preparation of stanna[*n*]troticenophanes (*n* = 1, 2): The stanna[1]- and stanna[2]troticenophanes **3** and **4** were prepared by salt elimination reactions of $[Ti(\eta^5\text{-}C_5H_4Li)(\eta^7\text{-}C_7H_6Li)]\cdot$pmdta (**2**) with $X_2Sn(Mes)_2$ (X = Cl, Br; Mes = 2,4,6-trimethylphenyl) and $Cl_2Sn_2tBu_4$, respectively (Scheme 2). These are the first fully characterized representatives of heteroleptic sandwich complexes featuring bridging Sn or Sn–Sn moieties. For complex **3**, several crystallizations from hexane were required to obtain pure samples and to remove the accompanying [(pmdta)LiX] (X = Cl, Br) salts completely—the bromide impurities stem from the preparation of $Cl_2Sn(Mes)_2$ from (Mes)MgBr and $SnCl_4$ (see below).[31] Clearly, the use of sterically demanding mesityl substituents at the tin atom is essential for the isolation of a strained stanna[1]troticenophane, since attempts to prepare analogous complexes by employment of other diorganotin halides Cl_2SnR_2 (R = Me, *n*Bu, Ph) furnished intractable mixtures of nondefined products.

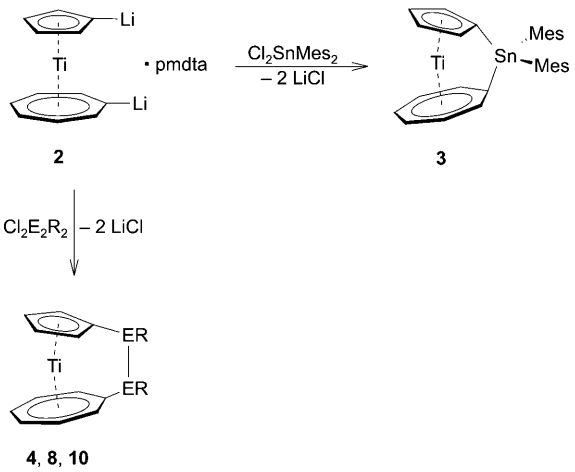

Scheme 2. Synthesis of [*n*]troticenophanes (*n* = 1, 2).

The ^{1}H NMR spectrum of **3** reveals a similar splitting pattern as that of $[Ti(\eta^5\text{-}C_5H_4)(C_7H_6)EMe_2]$ (E = Si, Ge).[20a,c] Two broad resonances are observed at $\delta = 5.17$ and 5.81 ppm, which can be assigned to the seven-membered-ring protons, whereas the C_5H_4 protons give rise to one broad signal at $\delta = 5.02$ ppm. The ^{13}C NMR spectrum shows seven signals for the sandwich unit in the range of $\delta = 69.0$–103.0 ppm, whereby the two signals at high field at 69.0 (C_7H_6) and 88.3 ppm (C_5H_4) can be unambiguously assigned to the *ipso*-carbon atoms. The bridging tin atom gives rise to a signal at −134.7 ppm in the ^{119}Sn NMR spectrum.

Although **3** could be isolated in analytically pure form (see Experimental Section), repeated attempts to obtain single crystals of **3** failed. Fortunately, crystallization of a contaminated sample of **3** from hexane at −30 °C produced usable crystals of **3**·[(pmdta)LiBr],[32] which allowed confirmation of the molecular structure of **3** by X-ray diffraction analysis (Figure 2). In agreement with the molecular structure of troticene (**1**),[33] the Ti–C distances to the seven-membered ring (2.185(3)–2.237(3) Å) are significantly shorter than those to the five-membered ring (2.301(3)–2.341(3) Å), thus indicating a stronger interaction between the metal and the C_7H_6 ligand.[18] The Ti–Sn distance found in **3** is 3.2379(6) Å, which is considerably greater than the sum of the covalent radii of Ti and Sn (2.77 Å).[34] This value is even larger than those found in $[CpTi(CNXyl)_4ER_3]$ (Xyl = xylene; $ER_3 = SnPh_3$: 2.9839(6); E = $SnMe_3$: 2.949(1) Å), which represent the longest Ti–Sn distances reported to date.[35] Thus, any significant interaction between the metal center and the heteroatom in **3** can be disregarded. As expected, the Ti–E distance increases in the order

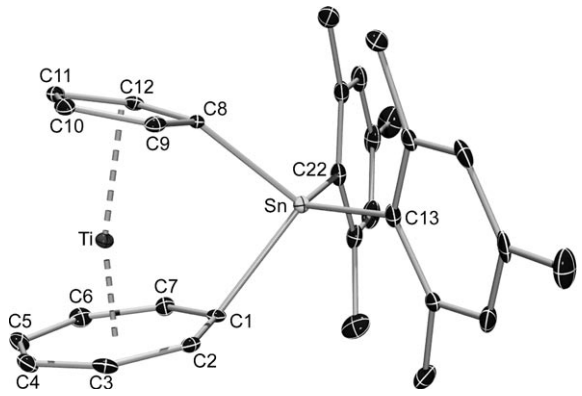

Figure 2. Molecular structure of $[Ti(\eta^5\text{-}C_5H_4)(\eta^7\text{-}C_7H_6)Sn(Mes)_2]$ (**3**) in **3**·[(pmdta)LiBr]. Hydrogen atoms and incorporated [LiBr(pmdta)] are omitted for clarity. Thermal ellipsoids are displayed at the 30% probability level. Selected bond lengths [Å] and angles [°]: Sn–C1 2.182(3), Sn–C8 2.167(3), Sn–C13 2.168(3), Sn–C22 2.165(4), Ti–C1 2.187(3), Ti–C2 2.185(3), Ti–C3 2.217(3), Ti–C4 2.237(3), Ti–C5 2.225(3), Ti–C6 2.216(3), Ti–C7 2.193(3), Ti–C8 2.301(3), Ti–C9 2.309(3), Ti–C10 2.340(3), Ti–C11 2.341(3), Ti–C12 2.306(3), Ti–X_{Cp} 1.981, Ti–X_{Cht} 1.480; X_{Cp}-Ti-X_{Cht} 165.7, $\alpha = 17.2$ (X_{Cp} = centroid of the C_5H_4 ring, X_{Cht} = centroid of the C_7H_6 ring).

Ti–Si (3.008 Å) < Ti–Ge (3.090 Å) < Ti–Sn (3.238 Å) owing to the larger size of Sn compared to Si and Ge. Accordingly, one could expect a less strained structure for **3** with respect to the silicon and germanium analogues.[20a,c] This is confirmed by a smaller dihedral angle $\alpha = 17.2°$ versus 24.1° in the sila[1]troticenophane and 22.9° in the germa[1]troticenophane, together with a larger X_{Cht}-Ti-X_{Cp} (X_{Cht} = centroid of the C_7H_6 ring, X_{Cp} = centroid of the C_5H_4 ring) angle δ (165.7° in **3** versus 160.5° and 161.0°). A detailed structural comparison of the degree of distortion for [1]troticenophanes and [1]ferrocenophanes is given in Table 1. Thus, it

Table 1. Structural parameters of [1]troticenophanes and [1]ferrocenophanes.

	[Ti(η⁵-C_5H_4)(η⁷-C_7H_6)ER_2]			[Fe(η⁵-C_5H_4)$_2ER_2$]		
ER_2	$SiMe_2$[a]	$GeMe_2$[b]	$SnMes_2$	$SiMe_2$[c]	$GeMe_2$[d]	$SnMes_2$[e]
α [°]	24.1	22.9	17.2	20.8(5)	19.0(9)	15.2(2)
β_{Cp} [°]	29.2	28.5	27.7	37.0(6)	36.8(7)	35.3(2)
β_{Cht} [°]	42.3	41.4	42.6	–	–	–
θ [°]	95.6	92.8	87.4	95.7(4)	91.7(3)	85.8(2)
δ [°]	160.5	161.0	165.7	164.7(8)	165.3(5)	167.6(2)

[a] Experimental values see ref. [20a]. [b] Experimental values see ref. [20c]. [c] Experimental values see ref. [2c]. [d] Experimental values see ref. [4b]. [e] Experimental values see ref. [4d].

can be concluded that **3** exhibits the least strained structure found so far for [1]troticenophanes. A similar trend has been observed for the corresponding sila-, germa-, and stanna[1]ferrocenophanes (Table 1). Comparison with other Mes_2Sn-bridged [1]metallocenophanes reveals that the tilt angle α decreases from [Ru(η⁵-C_5H_4)$_2$Sn(Mes)$_2$][9b] (20.6°) > **3** (17.2°) > [Fe(η⁵-C_5H_4)$_2$Sn(Mes)$_2$] (15.2°),[4d] accompanying an increase in the angle δ, following the order [Ru(η⁵-C_5H_4)$_2$Sn(Mes)$_2$] (164.5°) < **3** (165.7°) < [Fe(η⁵-C_5H_4)$_2$Sn-(Mes)$_2$] (167.6°). Accordingly, **3** adopts an intermediate position between the corresponding *ansa*-ferrocene and *ansa*-ruthenocene with regard to its deviation from an unstrained sandwich structure.

Stanna[2]ferrocenophanes represent a well-investigated class of compounds, and their use as potential precursors in metal-mediated distannation reactions has been demonstrated by Herberhold et al.[36] Recently, we reported the syntheses and reactivity of *ansa* half-sandwich complexes [M(η⁵-C_5H_4)$(CO)_3Sn_2tBu_4$] (M = Mo, W).[37] The salt elimination reaction between **2** and $Cl_2Sn_2tBu_4$ allowed for the isolation of the first heteroleptic sandwich complex featuring a Sn–Sn moiety as the *ansa* bridge. The ^{1}H NMR spectroscopic data of [Ti(η⁵-C_5H_4)(η⁷-C_7H_6)Sn_2tBu_4] (**4**) are fully consistent with the proposed structure and reveal five signals (δ = 5.23–5.88 ppm) for the aromatic CH groups and two singlets at $\delta = 1.43$ and 1.59 ppm for the nonequivalent *t*Bu groups. The latter show the expected sets of ^{117}Sn ($^3J_{H-117Sn} = 63.1$ and $^3J_{H-117Sn} = 62.7$ Hz) and ^{119}Sn ($^3J_{H-119Sn} = 66.0$ and $^3J_{H-119Sn} = 65.6$ Hz) satellites. By contrast, the long-range $^4J_{H-Sn}$ couplings are not resolved in the ^{1}H NMR spectrum, thus appearing as one set of satellites for both Sn nuclei. The ^{119}Sn NMR spectrum shows two distinct resonances at δ = −28.4 and −9.0 ppm, each surrounded by ^{117}Sn ($^1J_{119Sn-117Sn} = 1144.4$ Hz) and ^{119}Sn ($^1J_{119Sn-119Sn} = 1197.9$ Hz) satellites. X-ray diffraction analysis reveals two independent molecules in the asymmetric unit, which show only marginal differences in the structural parameters. Hence, only one of the molecular structures is discussed below (Figure 3). The distanna bridge in **4** has only negligible impact on the molecular geometry of the sandwich unit. Both aromatic rings adopt an almost coplanar orientation, indicated by the tilt angle α = 2.0° and the angle $\delta = 178.5°$ (Table 2). These values lie within the range of those reported for [Fe(η⁵-C_5H_4)$_2Sn_2Me_4$].[38]

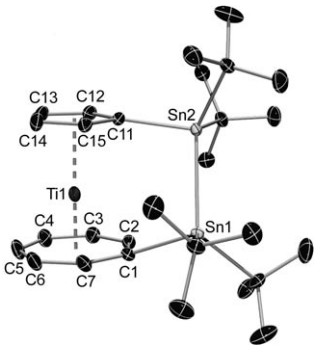

Figure 3. Molecular structure of [Ti(η⁵-C_5H_4)(η⁷-C_7H_6)Sn_2tBu_4] (**4**). For clarity, only one of the molecules in the asymmetric unit is shown and hydrogen atoms are omitted. Thermal ellipsoids are displayed at the 30% probability level. Selected bond lengths [Å] and angles [°]: Sn1–C1 2.175(5), Sn2–C11 2.162(5), Sn1–Sn2 2.8322(5), Ti–C1 2.219(5), Ti–C2 2.191(5), Ti–C3 2.208(6), Ti–C4 2.214(6), Ti–C5 2.212(6), Ti–C6 2.200(6), Ti–C7 2.198(6), Ti–C11 2.340(5), Ti–C12 2.322(6), Ti–C13 2.331(6), Ti–C14 2.332(6), Ti–C15 2.315(5), Ti–X_{Cp} 1.995, Ti–X_{Cht} 1.480; C1-Sn1-Sn2 95.5(2), C11-Sn2-Sn1 97.7(2), C1-Sn1-Sn2-C11 30.6(2) , X_{Cp}-Ti-X_{Cht} 178.5, $\alpha = 2.0$.

Table 2. Structural parameters of [*n*]troticenophanes (*n* = 2, 3).

	α [°]	β_{Cp} [°]	β_{Cht} [°]	γ [°]	δ [°]
4	2.0	6.3	18.7	30.6(2)	178.5
5[a]	10.6/9.8	8.2	3.0	−5.7(2)/7.9(2)	172.2/172.7
6	2.7	2.3	6.5	−32.0	177.4
8	14.7	14.5	28.0	42.4(2)	167.6
9	6.3	4.7	13.6	−7.4	174.9
10	4.2	7.1	20.6	−4.7(1)	176.7
11	0.7	5.8	11.9	−2.7	179.5

[a] Molecule 1/molecule 2.

Insertion reactions of stanna[*n*]troticenophanes (*n* = 1, 2): As repeatedly reported by our groups, *ansa*-Cht-Cp complexes are susceptible towards strain release by transition-metal-catalyzed ROP reactions, and it was shown that the complexes [M(η⁵-C_5H_4)(η⁷-C_7H_6)$SiMe_2$] (M = Ti, V, Cr) react with [Pt(PEt_3)$_3$] to undergo a regioselective insertion of the [Pt(PEt_3)$_2$] fragment into the Si–C_{ipso} bond between the silicon atom and the seven-membered ring.[20,24] Accordingly, the same reaction was investigated for complex **3**, and its treatment with equimolar amounts of [Pt(PEt_3)$_3$] in tolu-

ene at 60 °C for two days afforded the platinastanna[2]troticenophane **5** as a blue crystalline solid after recrystallization from hexane (Scheme 3).

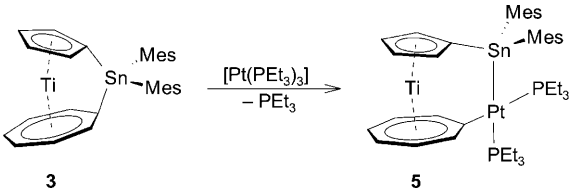

Scheme 3. Regioselective insertion of $[Pt(PEt_3)_2]$ into the Sn–C_{ipso} bond.

Compound **5** was fully characterized by multinuclear NMR spectroscopy and elemental analysis. The ^{31}P NMR spectrum (Figure 4) exhibits two signals at 9.93 ppm (*trans*

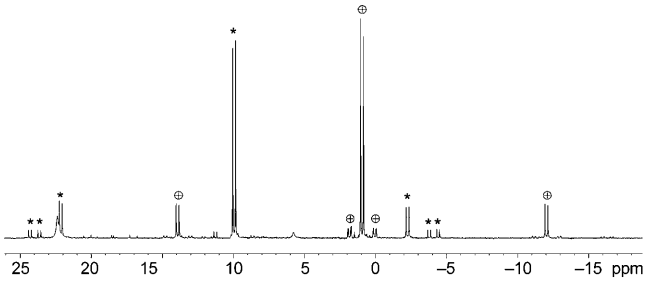

Figure 4. ^{31}P NMR spectrum (in C_6D_6) of **5**; all relevant signals (including ^{195}Pt, ^{119}Sn, and ^{117}Sn satellites) are denoted with * (for the phosphorus nucleus *trans* to Sn) or with ⊕ (for the phosphorus nucleus *cis* to Sn).

to Sn) and 0.94 ppm (*cis* to Sn), each flanked by ^{31}P–^{195}Pt and ^{31}P–$^{117/119}Sn$ satellites, thus suggesting a square-planar environment at the platinum atom. Because of ^{31}P–^{31}P coupling, each ^{31}P signal splits into doublets with $^2J_{31P-31P} = 16$ Hz. Furthermore, these signals show large ^{31}P–^{195}Pt coupling constants of 1978 and 2104 Hz, respectively. Comparison with the values determined for the corresponding platinasila- (998 and 2104 Hz) and platinagerma[2]troticenophanes (1647 and 2013 Hz)[20b,c] indicates that the difference between the coupling constants decreases in the order Si > Ge > Sn, which reveals that the stannyl group has a significantly smaller *trans* influence than the germyl and silyl substituents. In addition, the observation of $^{117/119}Sn$ satellites with $^2J_{31P-117Sn}$ (*trans*) = 2222, $^2J_{31P-119Sn}$ (*trans*) = 2327, $^2J_{31P-117Sn}$ (*cis*) = 128, and $^2J_{31P-119Sn}$ (*cis*) = 160 Hz confirms the presence of a direct platinum–tin bond in **5**.[39] Consequently, the ^{119}Sn NMR spectrum of **5** shows a doublet of doublets at $\delta = -152.5$ ppm, because of coupling with the *trans*- and *cis*-phosphorus nuclei. Finally, the ^{119}Sn NMR signal is flanked by ^{195}Pt satellites with a large $^1J_{119Sn-195Pt}$ coupling constant of 13302 Hz.

The structural assignments based on NMR spectroscopic data were confirmed by X-ray diffraction analysis. The asymmetric unit of **5** contains two independent molecules with very similar structural characteristics, and the molecular structure of molecule 1 is shown in Figure 5. As expected, the introduction of a $[Pt(PEt_3)_2]$ unit results in significant relief of strain in comparison with the structure of **3**, as indi-

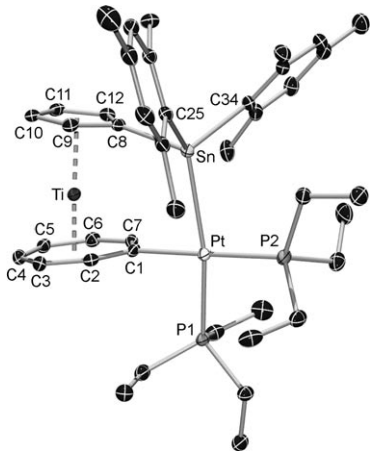

Figure 5. Molecular structure of one of the two independent molecules of $[Ti(\eta^5\text{-}C_5H_4)(\eta^7\text{-}C_7H_6)Sn(Mes)_2Pt(PEt_3)_2]$ (**5**). Hydrogen atoms are omitted for clarity. Selected bond lengths [Å] and angles [°]: Pt–C1 2.102(4), Pt–P1 2.3385(10), Pt–P2 2.3016(10), Pt–Sn 2.6332(3), Sn–C8 2.187(4), Sn–C25 2.217(4), Sn–C34 2.215(4), Ti–C1 2.221(4), Ti–C2 2.187(4), Ti–C3 2.210(4), Ti–C4 2.227(4), Ti–C5 2.234(4), Ti–C6 2.215(4), Ti–C7 2.186(4), Ti–C8 2.300(4), Ti–C9 2.308(4), Ti–C10 2.345(4), Ti–C11 2.356(4), Ti–C12 2.308(4), Ti–X_{Cp} 1.985, Ti–X_{Cht} 1.484; C1-Pt-P1 82.50(10), P1-Pt-P2 98.82(4), C1-Pt-Sn 83.30(10), P2-Pt-Sn 95.56(3), C8-Sn-Pt 112.12(10), C34-Sn-Pt 122.33(10), C25-Sn-Pt 110.49(10), C8-Sn-C25 106.03(15), C8-Sn-C34 94.07(14), C25-Sn-C34 109.78(15), X_{Cp}-Ti-X_{Cht} 172.2, $\alpha = 10.6$.

cated by tilt angles $\alpha = 10.6°$ (molecule 1) and $\alpha = 9.8°$ (molecule 2) together with the deformation angles $\delta = 172.2°$ and 172.7° (Table 2). Comparison with the structures of Si–Pt-bridged *ansa*-Cht-Cp complexes $[M(\eta^5\text{-}C_5H_4)(\eta^7\text{-}C_7H_6)SiMe_2\text{–}Pt(PEt_3)_2]$ (M = Ti: $\alpha = 13.5°$, $\delta = 169.1°$;[20c] M = V: $\alpha = 10.6°$, $\delta = 171.9°$;[20b] M = Cr: $\alpha = 7.51(7)°$, $\delta = 174.9°$)[24b] reveals a similar degree of distortion, even though the deviation from an unstrained sandwich structure is clearly less pronounced for **3** than for its platinasila[2]troticenophane congener, in agreement with the incorporation of a larger tin atom. Due to the *trans* influence of the stannyl substituent, the Pt–P1 distances (2.3385(10) and 2.3359(10) Å) in both molecules are greater than the Pt–P2 distances (2.3016(10) and 2.3129(10) Å). Finally, the Pt–Sn and Pt–C1 bond lengths in **5** (2.6332(3)/2.6518(3) and 2.102(4)/2.093(4) Å) fall in the expected ranges and are comparable to those found in the corresponding platinastanna[2]ferrocenophane (2.6065(4) and 2.034(4) Å).[4d]

It has been shown that systems such as $[Fe(\eta^5\text{-}C_5H_4)_2Sn_2Me_4]$ and $[M(\eta^5\text{-}C_5H_4)(CO)_3Sn_2tBu_4]$ (M = W, Mo) readily undergo insertion reactions in the presence of group 16 elements.[37,40] Thus, $[Ti(\eta^5\text{-}C_5H_4Sn tBu_2)(\eta^7\text{-}C_7H_6Sn tBu_2)E]$ (**6**: E = S; **7**: E = Se) were obtained by reaction of **4** with elemental sulfur and selenium in C_6D_6 at elevated temperatures (50 and 60 °C), respectively (Scheme 4). It should be noted that in the case of **7**, the insertion occurs

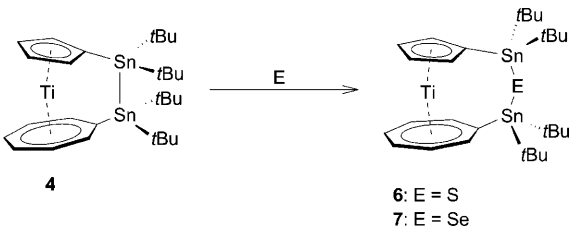

Scheme 4. Insertion of S and Se into $[Ti(\eta^5\text{-}C_5H_4)(\eta^7\text{-}C_7H_6)Sn_2tBu_4]$ (**4**).

only in the presence of red selenium, whereas the gray modification does not react.

The oxidative addition of **4** to elemental chalcogens is accompanied by a downfield shift in the ^{119}Sn NMR spectra with respect to **4** (**6**: $\delta = 25.54$ and 42.93 ppm; **7**: $\delta = 20.77$ and 47.73 ppm). Because of $J_{Sn-77Se}$ coupling, the ^{119}Sn NMR signals of **7** are flanked by satellites with coupling constants of 1431.4 and 1364.2 Hz. Compound **6** crystallizes in the tetragonal space group $I4_1/a$, and the asymmetric unit contains three independent molecules. For simplicity reasons, only one of the molecular structures is discussed below (Figure 6). Most of the geometrical parameters of **4** and **6** are comparable. The insertion of S into the Sn–Sn bond only slightly affects the sandwich geometry observed in the precursor **4** (Table 2). The C_{ipso}–Sn bond lengths lie in the same range for both **4** and **6**, and the aromatic ligands are still roughly coplanar. However, in contrast to **4**, **6** exhibits a decreased distortion at the seven-membered ring, emphasized by the reduction of $\beta = 6.5°$ versus $\beta = 18.7°$ in **4**. Hence, even though $\alpha = 2.7°$ and $\delta = 177.4°$ are almost unaffected, the decrease of β clearly indicates a reduced ring strain. Because of the steric requirements of the triatomic bridge, the Sn atom bound to the C_5H_4 moiety resides above the ring plane.

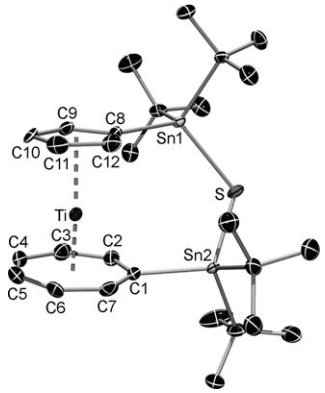

Figure 6. Molecular structure of $[Ti(\eta^5\text{-}C_5H_4SntBu_2)(\eta^7\text{-}C_7H_6SntBu_2)S]$ (**6**). For clarity, only one of the molecules in the asymmetric unit is shown and hydrogen atoms are omitted. Selected bond lengths [Å] and angles [°]: S–Sn1 2.4232(15), S–Sn2 2.4202(15), Sn1–C8 2.147(6), Sn2–C1 2.136(6), Ti–C1 2.195(6), Ti–C2 2.205(6), Ti–C3 2.211(6), Ti–C4 2.222(6), Ti–C5 2.220(7), Ti–C6 2.222(6), Ti–C7 2.197(6), Ti–C8 2.340(6), Ti–C9 2.362(7), Ti–C10 2.346(7), Ti–C11 2.338(7), Ti–C12 2.320(7), Ti–X_{Cp} 2.0016, Ti–X_{Cht} 1.4876; C1-Sn2-S 107.3(2), C8-Sn1-S 116.9(2), Sn1-S-Sn2 112.0(1), X_{Cp}-Ti-X_{Cht} 177.4, $\alpha = 2.7$.

Synthesis of the bora[2]troticenophane 8: Bora[2]troticenophane **8** was prepared by a similar procedure to that described for complexes **3** and **4** by using $[Ti(\eta^5\text{-}C_5H_4Li)(\eta^7\text{-}C_7H_6Li)]\cdot$pmdta and $Cl_2B_2(NMe_2)_2$ (Scheme 2). Complex **8** was isolated in good yields as a blue solid after recrystallization from Et_2O at −30 °C. As expected, the introduction of a B–B bridge results in a splitting of the ^{1}H NMR spectroscopic resonances of the five-membered ring into two pseudotriplets ($\delta = 5.04$ and 5.37 ppm), and two multiplets at $\delta =$ 5.26 and 5.85 ppm are observed for the seven-membered ring. Previous studies of related systems suggest a correlation of molecular ring strain in [*n*]metalloarenophanes and the separation of the ^{1}H NMR signals of the C_5H_4 moiety.[3a,5b,c,26] However, this is not the case for strained [*n*]troticenophanes, and thus $[Ti(\eta^5\text{-}C_5H_4)(\eta^7\text{-}C_7H_6)SiMe_2]$ exhibits only one related resonance for the five-membered ring.[20a,24c] Because of chemical nonequivalence and hindered rotation about the B=N double bond in **8**, four resonances are detected for the Me groups in both the ^{1}H and ^{13}C NMR spectra. In agreement with the chromium congener, only five resonances are observed for the aromatic carbon atoms, which is attributable to the quadrupolar moment of the boron nuclei.[24a] In addition, the ^{11}B NMR spectrum shows two signals at $\delta = 42.0$ and 45.5 ppm.

To authenticate the formation of **8**, its solid-state structure was determined by X-ray diffraction analysis (Figure 7). Compound **8** crystallizes in the orthorhombic space group $P2_12_12_1$. Similar to the crystal structure of troticene,[41] the metal–carbon distances to the seven-membered ring (2.1900(16)–2.2272(17) Å) are significantly shorter than those to the five-membered ring (2.3095(16)–2.3446(17) Å). This is a well-known phenomenon that has been ascribed to strong metal–ligand δ interactions.[18] Additionally, the tilt angle α decreases significantly from bora[2]troticenophane

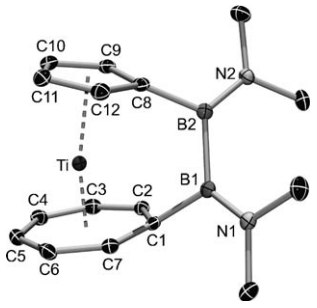

Figure 7. Molecular structure of $[Ti(\eta^5\text{-}C_5H_4)(\eta^7\text{-}C_7H_6)B_2(NMe_2)_2]$ (**8**). Hydrogen atoms are omitted for clarity. Selected bond lengths [Å] and angles [°]: C1–B1 1.603(2), C8–B2 1.594(2), B1–N1 1.399(2), B2–N2 1.395(2), B1–B2 1.728(2), Ti–C1 2.1914(15), Ti–C2 2.1900(16), Ti–C3 2.2219(17), Ti–C4 2.2248(17), Ti–C5 2.2272(17), Ti–C6 2.2206(16), Ti–C7 2.2049(16), Ti–C8 2.3193(16), Ti–C9 2.3305(16), Ti–C10 2.3446(17), Ti–C11 2.3405(18), Ti–C12 2.3095(16), Ti–X_{Cp} 1.9880, Ti–X_{Cht} 1.4778; C1-B1-B2 110.7(2), B2-B1-N1 127.2(1), N1-B1-C1 121.2(1), C8-B2-B1 111.7(2), B1-B2-N2 127.6(1), N2-B2-C8 120.3(1), C1-B1-B2-C8 −42.0(2), X_{Cp}-Ti-X_{Cht} 167.6, $\alpha = 14.7$.

(14.7°) to bora[2]trovacenophane[23] (11.4°) and bora[2]trochrocenophane[24a] (8.9°), which is a consequence of the interannular distances in troticene (3.48 Å), trovacene (3.38 Å) and trochrocene (3.26 Å), respectively.[7,16,19] In contrast to the tilt angle α, the deformation angles δ significantly widen from $[Ti(\eta^5\text{-}C_5H_4)(\eta^7\text{-}C_7H_6)B_2(NMe_2)_2]$ (167.6°) to $[V(\eta^5\text{-}C_5H_4)(\eta^7\text{-}C_7H_6)B_2(NMe_2)_2]$[23] (171.1°) and $[Cr(\eta^5\text{-}C_5H_4)(\eta^7\text{-}C_7H_6)B_2(NMe_2)_2]$[24a] (173.1°). In addition, the boron atoms show a typical trigonal planar geometry (Σ= 359° and 360°) with C-B-B angles of 111.7(2)° and 110.7(2)°.

Boron–boron bond cleavage of $[Ti(\eta^5\text{-}C_5H_4)(\eta^7\text{-}C_7H_6)B_2(NMe_2)_2]$ (8): B–B bonds are susceptible to oxidative addition reactions to low-valent transition-metal complexes, thus affording bis-boryl species,[23,24a,42] which prompted us to investigate whether **8** reacts with stoichiometric amounts of $[Pt(PEt_3)_3]$ at elevated temperatures to form $[Ti(\eta^5\text{-}C_5H_4BNMe_2)(\eta^7\text{-}C_7H_6BNMe_2)Pt(PEt_3)_2]$ (**9**) (Scheme 5). After four days, **9** could be isolated as a blue solid in good yields.

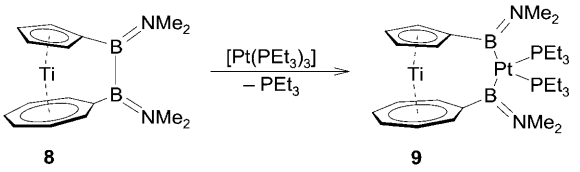

Scheme 5. Insertion of the $[Pt(PEt_3)_2]$ fragment into **8**.

The ^{1}H NMR spectroscopic data support the formulation as a C_1-symmetric compound, in which the incorporation of a $[Pt(PEt_3)_2]$ fragment entails a further splitting of the proton resonances into four distinct signals for each aromatic ring system. Compared to **8**, the ^{11}B NMR resonances are lowfield-shifted to δ = 57.6 and 62.7 ppm, which is in the same range as observed for diboraplatina[3]trochrocenophane (δ = 60.6 and 67.0 ppm).[24a] A similar trend is observed for the ^{31}P NMR resonances at δ = 10.0 and 10.7 ppm that are flanked by ^{195}Pt satellites with characteristic coupling constants of 1062.6 and 1171.0 Hz, respectively. Again, these values are in excellent agreement with those found for related species such as $[Cr(\eta^5\text{-}C_5H_4BNMe_2)(\eta^7\text{-}C_7H_6BNMe_2)Pt(PEt_3)_2]$,[24a] $[Fe(\eta^5\text{-}C_5H_4BNMe_2)_2Pt(PEt_3)_2]$, and $[Cr(\eta^6\text{-}C_6H_5BNMe_2)_2Pt(PEt_3)_2]$.[30a] Crystallization of **9** from a saturated hexane solution at −30°C afforded blue crystals that were suitable for X-ray diffraction (Figure 8). As expected, the insertion of a $[Pt(PEt_3)_2]$ fragment into the B–B bond results in a decrease of ring strain with respect to **8**, reflected by the smaller tilt angle α = 6.3° (Table 2). In contrast to similar complexes, the aromatic rings still show substantial deviation from a parallel arrangement. However, the boron atoms feature a planar environment (Σ = 359 and 360°), whereas the platinum center adopts a distorted square-planar geometry. All significant parameters such as the Pt–P bond lengths (2.3373(4) and 2.3469(5) Å), the Pt–B distances (2.118(2) and 2.112(2) Å), and the B-Pt-B

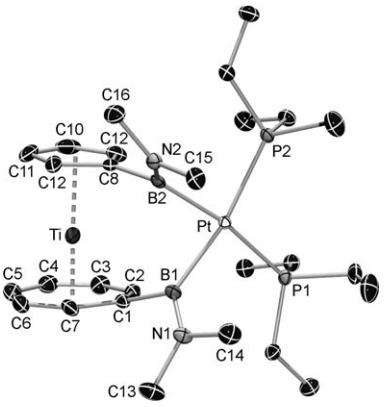

Figure 8. Molecular structure of $[Ti(\eta^5\text{-}C_5H_4BNMe_2)(\eta^7\text{-}C_7H_6BNMe_2)Pt(PEt_3)_2]$ (**9**). Hydrogen atoms and hexane incorporated into the crystal lattice are omitted for clarity. Selected bond lengths [Å] and angles [°]: C1–B1 1.606(3), C8–B2 1.589(3), B1–N1 1.417(2), B2–N2 1.422(3), B1–Pt 2.118(2), B2–Pt 2.112(2), P1–Pt 2.3373(4), P2–Pt 2.3469(5), Ti–C1 2.194(2), Ti–C2 2.179(2), Ti–C3 2.214(2), Ti–C4 2.218(2), Ti–C5 2.215(2), Ti–C6 2.209(2), Ti–C7 2.189(2), Ti–C8 2.328(2), Ti–C9 2.307(2), Ti–C10 2.327(2), Ti–C11 2.309(2), Ti–C12 2.300(2), Ti–X_{Cp} 1.968, Ti–X_{Cht} 1.476; B1-Pt-B2 77.24(7), B1-Pt-P1 94.02(5), P1-Pt-P2 98.53(2), P2-Pt-B2 90.25(5), B1-Pt-P2 167.45(5), B2-Pt-P1 170.44(5), X_{Cp}-Ti-X_{Cht} 174.9, α = 6.3.

(77.2(1)°) and P-Pt-P (98.5(1)°) angles lie within previously reported ranges.[24a,30a]

Syntheses of silicon-bridged [*n*]troticenophanes (*n* = 2, 3): Both the [2]troticenophane **10** (Scheme 2) and the [3]troticenophane **11** (Scheme 6) were prepared by treatment of **2** at low temperature with $Cl_2Si_2Me_4$ and $(ClSiMe_2)_2CH_2$, respectively. After chromatography, **10** and **11** were isolated in yields of 63 and 40%.

Scheme 6. Synthesis of $[Ti(\eta^5\text{-}C_5H_4SiMe_2)(\eta^7\text{-}C_7H_6SiMe_2)CH_2]$ (**11**).

The constitution of **10** was confirmed by multinuclear NMR data and X-ray diffraction (Figure 9). In general, the extent of molecular strain depends on several parameters such as the nature of the metal center, the number of bridging elements, and their covalent radii. Hence, it is clearly a consequence of the smaller covalent radius of Si compared to Sn that the aromatic ligands in $[Ti(\eta^5\text{-}C_5H_4)(\eta^7\text{-}C_7H_6)Si_2Me_4]$ (**10**) show a much larger deviation from the coplanar arrangement than in **4** (Table 2). Furthermore, the tilt angle α = 4.2° is larger than those found in the corresponding sila[2]trochrocenophanes (2.6(2)°) and sila[2]trovacenophanes (3.8(3)°),[16,24b] as a consequence of the greater interannular distance in troticene. The more pronounced

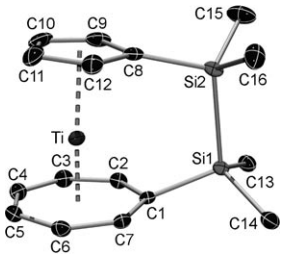

Figure 9. Molecular structure of $[Ti(\eta^5\text{-}C_5H_4)(\eta^7\text{-}C_7H_6)Si_2Me_4]$ (**10**). Hydrogen atoms are omitted for clarity. Thermal ellipsoids are displayed at the 30% probability level. Selected bond lengths [Å] and angles [°]: Si1–C1 1.883(2), Si2–C8 1.876(3), Si1–Si2 2.344(9), Ti–C1 2.200(2), Ti–C2 2.200(2), Ti–C3 2.214(2), Ti–C4 2.216(3), Ti–C5 2.209(2), Ti–C6 2.212(2), Ti–C7 2.199(2), Ti–C8 2.336(3), Ti–C9 2.318(3), Ti–C10 2.328(3), Ti–C11 2.337(3), Ti–C12 2.325(3), Ti–X_{Cp} 1.991, Ti–X_{Cht} 1.479; C1-Si1-Si2 105.2(1), C8-Si2-Si1 106.3(1), C1-Si1-Si2-C8 −4.7(1), X_{Cp}-Ti-X_{Cht} 176.7, $\alpha = 4.2$.

ring strain is also confirmed by the deformation angle $\delta = 176.7°$. However, it should be kept in mind that these parameters still suggest a rather unstrained molecule. This is also supported by the ^{13}C NMR spectroscopic data. The *ipso*-carbon atoms of both aromatic rings do not show the characteristic upfield shift that was observed for highly strained sila[1]metalloarenophanes such as $[M(\eta^5\text{-}C_5H_4)(\eta^7\text{-}C_7H_6)SiR_2]$ (M = Ti, Cr),[20b,c,24b,c] $[Cr(\eta^6\text{-}C_6H_5)_2SiR_2]$,[14c,d] and $[Fe(\eta^5\text{-}C_5H_4)_2SiR_2]$.[4]

The [3]troticenophane **11** was also characterized in solution and in the solid state. As expected, the incorporation of a triatomic bridge in $[Ti(\eta^5\text{-}C_5H_4SiMe_2)(\eta^7\text{-}C_7H_6SiMe_2)CH_2]$ (**11**) does not result in a substantial deviation of the geometry of the aromatic rings in comparison to troticene. Thus, ^1H NMR spectroscopic data are in excellent agreement with those obtained for the 1,1′-disubstituted compound $[Ti(\eta^5\text{-}C_5H_4SiMe_3)(\eta^7\text{-}C_7H_6SiMe_3)]$,[43] and show two signals for the C_5H_4 protons at $\delta = 5.02$ and 5.10 ppm and one multiplet for the C_7H_6 moiety at $\delta = 5.53$ ppm. In addition, deshielded resonances of the *ipso*-carbon atoms are observed in the ^{13}C NMR spectrum (C_5H_4: 110.3 ppm; C_7H_6: 94.9 ppm), which is consistent with the unstrained character of **11**.

The molecular structure of **11** in the solid state was determined by X-ray diffraction (Figure 10). Again, the carbon–metal distances to the seven-membered ring (2.200(5)–2.250(4) Å) are significantly shorter than those to the five-membered ring (2.298(2)–2.302(4) Å). As already indicated by ^{13}C NMR data, both ring ligands adopt an almost coplanar arrangement, which is reflected by the angles $\alpha = 0.7°$ and $\delta = 179.5°$, and the bridging C and Si atoms exhibit a distorted tetrahedral geometry. The most important geometrical parameters of compounds **4**–**6** and **8**–**11** are summarized in Table 2.

UV/Vis spectroscopy: To gain more information on the electronic structure of [*n*]troticenophanes, solution UV/Vis spectra were collected in CH_2Cl_2 for the species **3**, **4**, **8**, **10**, and **11**. As reported before, the lowest-energy band in **1** ($\lambda = 696$ nm) is ascribed to a one-electron HOMO–LUMO transition. However, the introduction of an *ansa* bridge reduces the molecular symmetry and thus lifts the degeneracy of the HOMO orbitals, which leads to a small increase of the HOMO–LUMO gap.[18,20] Therefore, $[Ti(\eta^5\text{-}C_5H_4)(\eta^7\text{-}C_7H_6)SiMe_2)]$ shows a significant blueshift ($\lambda = 663$ nm) in the UV/Vis spectrum with respect to **1**.[20] This is in contrast to the trend reported for [*n*]trochrocenophanes and [*n*]ferrocenophanes, which exhibit a lowering of the HOMO–LUMO gap as the tilt angle increases. Thus, the visible bands of complexes **3**, **4**, **8**, **10**, and **11** are expected to lie between those of **1** and $[Ti(\eta^5\text{-}C_5H_4)(\eta^7\text{-}C_7H_6)SiMe_2)]$. Hence, **3** displays a maximum at $\lambda = 667$ nm, similar to that of $[Ti(\eta^5\text{-}C_5H_4)(\eta^7\text{-}C_7H_6)SiMe_2)]$, which indicates the strained nature of the complex. By contrast, the introduction of a Sn–Sn bridge in **4** results in an only marginally distorted structure, concomitant with a less pronounced blueshift ($\lambda = 681$ nm). Despite the fact that the aromatic ligands in **11** adopt an almost perfectly parallel orientation, its visible band is observed at $\lambda = 666$ nm, which suggests the existence of a highly strained molecule. It should be noted that boron-bridged trochrocenophanes and ferrocenophanes, such as $[Cr(\eta^5\text{-}C_5H_4)(\eta^7\text{-}C_7H_6)BN(SiMe_3)_2]$ and $[Fe(\eta^5\text{-}C_5H_4)_2BN(SiMe_3)_2]$, also show a deviant behavior compared to other [*n*]trochrocenophanes and [*n*]ferrocenophanes, associated with the strong electronic influence of the B=N π system.[3a,24c] However, in the absence of such a π system the considerable blueshift of **11** cannot be explained so far. Compounds **8** and **10** exhibit visible bands at $\lambda = 675$ and 678 nm, respectively, which indicates only moderate distortion of these compounds, though a possible influence of the B=N π system on the electronic structure of the sandwich unit in **8** cannot be excluded.

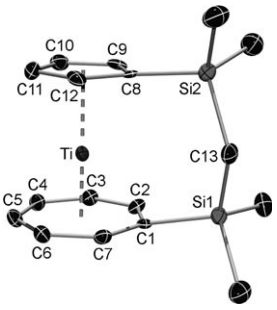

Figure 10. Molecular structure of $[Ti(\eta^5\text{-}C_5H_4SiMe_2)(\eta^7\text{-}C_7H_6SiMe_2)CH_2]$ (**11**). Hydrogen atoms are omitted for clarity. Thermal ellipsoids are displayed at the 30% probability level. Selected bond lengths [Å] and angles [°]: Si1–C13 1.895(3), Si2–C13 1.883(5), C1–Si1 1.895(3), C8–Si2 1.897(3), Ti–C1 2.208(3), Ti–C2 2.200(5), Ti–C3 2.200(5), Ti–C4 2.232(5), Ti–C5 2.234(5), Ti–C6 2.250(4), Ti–C7 2.245(4), Ti–C8 2.302(2), Ti–C9 2.301(2), Ti–C10 2.298(2), Ti–C11 2.298(3), Ti–C12 2.300(2), Ti–X_{Cp} 1.9463, Ti–X_{Cht} 1.5034; C1-Si1-C13 113.2(2), C8-Si2-C13 109.4(2), Si1-C13-Si2 120.1(2), X_{Cp}-Ti-X_{Cht} 179.5, $\alpha = 0.7$.

Conclusion

Herein, the preparation of [*n*]troticenophanes ($n = 1, 2, 3$), through reaction of $[Ti(\eta^5\text{-}C_5H_4Li)(\eta^7\text{-}C_7H_6Li)]\cdot$pmdta (**2**) with the appropriate element dihalides, has been presented. The incorporation of a Sn (**3**) and a Sn–Sn (**4**) bridge represents the first examples of heteroleptic sandwich complexes featuring this structural motif. The solid-state structure of **3**

highlights the strained character, with a tilt angle $\alpha = 17.2°$ appreciably less than that for its silicon- and germanium-bridged congeners. Treatment of **3** with Pt^0 resulted in the insertion of a $[Pt(PEt_3)_2]$ moiety into the C_{ipso}–Sn bond, exclusively at the seven-membered ring (**5**). This emphasizes the strained character of **3** and its potential suitability as a precursor in ROP reactions. In addition, **4** was prone to undergo insertion reactions in the presence of group 16 elements (S and Se) at elevated temperatures, yielding compounds **6** and **7**. Thus, due to their versatile reactivity pattern, these novel stanna[*n*]troticenophanes can be regarded as model compounds for further transformation reactions. In addition, the bora[2]troticenophane **8** was synthesized and characterized, and it was demonstrated that **8** represents the most strained system in the series going from bora[2]troticenophane (14.7°) to bora[2]trovacenophane (11.4°) and bora[2]trochrocenophane (8.9°). Furthermore, the insertion of $[Pt(PEt_3)_2]$ into the B–B bond supports the suitability of **8** and **9** for further functionalization reactions, for example the diboration of alkynes. In contrast to **8**, the disila-bridged [2]troticenophane exhibits a less distorted geometry with a tilt angle $\alpha = 4.2°$, and compound **11**, featuring a triatomic bridge, is best considered as an unstrained molecule. The electronic structures of **3**, **4**, **8**, **10**, and **11** were also investigated by UV/Vis spectroscopy. As previously reported, the maximum of the lowest-energy bands shows a characteristic blueshift with respect to troticene. However, the UV/Vis data did not reveal any distinct correlation between the degree of molecular distortion and the absorption maximum. Thus, both the highly strained complex **3** and the unstrained system **11** display bands in the same range as [Ti(η^5-C_5H_4)(η^7-C_7H_6)$SiMe_2$)].

Experimental Section

General procedures: All operations were performed under an atmosphere of argon, by using either standard Schlenk techniques or in a glovebox. Solvents were dried by standard procedures. $Cl_2Si_2Me_4$ was purchased from Aldrich and used without further purification. NaCp,[44] $[TiCl_4(thf)_2]$,[45] [Ti(η^5-C_5H_4Li)(η^7-C_7H_6Li)]·pmdta (**2**),[25] $Cl_2Sn(Mes)_2$,[31] $Cl_2Sn_2tBu_4$,[46] $(ClSiMe_2)_2CH_2$,[47] $Cl_2B_2(NMe_2)_2$,[48] and $[Pt(PEt_3)_3]$[49] were prepared according to published procedures. The NMR spectra were recorded on a Bruker DRX 400 MHz or a Bruker AV 500 FT-NMR spectrometer. ^1H and ^{13}C NMR spectra were referenced to external TMS via the residual protons of the solvent (^1H) or the solvent itself (^{13}C). ^{11}B NMR spectra were referenced to $BF_3{\cdot}OEt_2$, ^{29}Si NMR spectra to external TMS, ^{31}P NMR spectra to 85% H_3PO_4 and ^{119}Sn NMR spectra to Me_4Sn. Coupling constants (*J*) are reported in Hertz (Hz), and splitting patterns are indicated as s (singlet), d (doublet), t (triplet), m (mulitplet), and br (broad). UV/Vis spectra were recorded on a Shimadzu UV Mini 1240 UV/Vis photometer. Elemental analysis (C, H, N) was performed by combustion and gas chromatographic analysis with an Elementar Vario MICRO elemental analyzer.

[Ti(η^5-C_5H_5)(η^7-C_7H_7)] (1): A solution of NaCp (4.20 g, 47.68 mmol) in THF (40 mL) was added to a solution of $[TiCl_4(thf)_2]$ (8.00 g, 23.96 mmol) in THF (40 mL) at 0 °C. After complete addition, the reaction mixture was allowed to reach ambient temperature and stirred overnight. During this time, the color changed to red. The resulting suspension was added over a period of 1 h to a mixture of Mg turnings (2.04 g, 83.92 mmol), cycloheptatriene (5 mL), and catalytic amounts of $FeCl_3$ in THF (20 mL) at 0 °C. Subsequently, the suspension was allowed to warm to room temperature. After stirring overnight, all volatiles were removed in vacuo and the resulting residue was sublimed at 130 °C and 10^{-3} mbar. [Ti(η^5-C_5H_5)(η^7-C_7H_7)] (2.50 g, 12.25 mmol, 51%) was obtained as a crystalline blue solid. ^1H NMR (500 MHz, C_6D_6, 297 K): $\delta = 4.91$ (s, 5H; C_5H_5), 5.43 ppm (s, 7H; C_7H_7); $^{13}C\{^1H\}$ NMR (126 MHz, C_6D_6, 297 K): $\delta = 86.4$ (s, *C*H, C_7H_7), 97.0 ppm (s, *C*H, C_5H_5); elemental analysis calcd (%) for $C_{12}H_{12}Ti$ (204.09): C 70.62, H 5.93; found: C 70.46, H 5.95.

[Ti(η^5-C_5H_4)(η^7-C_7H_6)Sn(Mes)$_2$] (3): A suspension of **1** (0.25 g, 0.64 mmol) was prepared in hexane (20 mL) and cooled to −78 °C for 10 min. A suspension of Cl_2SnMes_2 (0.23 g, 0.64 mmol) in hexane (10 mL) was slowly added at −78 °C with continuous stirring. The reaction mixture was slowly warmed to room temperature and, after stirring for 2 h, it was filtered through celite. The solvent of the filtrate was evaporated under reduced pressure and the resultant blue-green solid was dried for 6 h under high vacuum. After recrystallization (2–3 times) from a hexane solution at −30 °C, the desired compound was obtained in pure form as a blue crystalline solid (0.21 g, 0.38 mmol, 59%). ^1H NMR (400 MHz, C_6D_6, 297 K): $\delta = 2.18$ (br, 6H; Me_{para}, Mes), 2.94 (s, $J_{H-117/119Sn} = 7.5$ Hz, 12H; Me_{ortho}, Mes), 5.02 (m, 4H; C_5H_4), 5.17 (m, 2H; C_7H_6), 5.81 (br m, 4H; C_7H_6), 6.89 ppm (s, $J_{H-117/119Sn} = 21$ Hz, 4H; C*H*, Mes); $^{13}C\{^1H\}$ NMR (100 MHz, C_6D_6, 297 K): $\delta = 21.4$ (s, Me_{para}, Mes), 26.5 (s, $J_{C-117/119Sn} = 37.5$ Hz, Me_{ortho}, Mes), 69.0 (s, C_{ipso}, C_7H_6), 88.3 (s, C_{ipso}, C_5H_4), 89.9 (s, *C*H, C_7H_6), 91.5 (s, *C*H, C_7H_6), 99.6 (s, *C*H, C_7H_6), 101.1 (s, *C*H, C_5H_4), 103.0 (s, *C*H, C_5H_4), 129.6 (s, $J_{C-117/119Sn} = 49.5$ Hz, C_{ipso}, Mes), 135.6 (s, *C*H, Mes), 139.9 (s, C_{para}, Mes), 146.6 ppm (s, $J_{C-117/119Sn} = 38$ Hz, C_{ortho}, Mes); $^{119}Sn\{^1H\}$ NMR (149 MHz, C_6D_6, 297 K): $\delta = -134.7$ ppm (s); λ_{max} (ε) = 667 nm (97 L mol^{-1} cm^{-1}); elemental analysis calcd (%) for $C_{30}H_{32}SnTi$ (559.15): C 64.44, H 5.76; found: C 64.47, H 6.11.

[Ti(η^5-C_5H_4)(η^7-C_7H_6)Sn_2tBu_4] (4): Over a period of 1 h, a solution of $Cl_2Sn_2tBu_4$ (0.87 g, 1.62 mmol) in hexane (10 mL) was added to a slurry of [Ti(η^5-C_5H_4Li)(η^7-C_7H_6Li)]·pmdta (0.60 g, 1.54 mmol) in hexane (15 mL) at −78 °C. Subsequently, the reaction mixture was allowed to reach ambient temperature and was stirred overnight. During that time a white precipitate formed and the color of the suspension turned to blue. After the solid had settled, the solution was filtered and the solvent of the filtrate was removed under reduced pressure. [Ti(η^5-C_5H_4)(η^7-C_7H_6)Sn_2tBu_4] (0.61 g, 0.92 mmol, 59%) was isolated as a blue solid after chromatography over alumina activity grade V with hexane as eluent. ^1H NMR (500 MHz, C_6D_6, 297 K): $\delta = 1.43$ (s, $J_{H-117Sn} = 63.1$, $J_{H-119Sn} = 66.0$, $J_{H-117/119Sn} = 5.4$ Hz, 18H; CMe_3), 1.59 (s, $J_{H-117Sn} = 62.7$, $J_{H-119Sn} = 65.6$, $J_{H-117/119Sn} = 5.7$ Hz, 18H; CMe_3), 5.23 (m, 2H; C_5H_4), 5.44 (m, 2H; C_5H_4), 5.49 (m, 2H; C_7H_6), 5.68 (m, 2H; C_7H_6), 5.88 ppm (m, 2H; C_7H_6); $^{13}C\{^1H\}$ NMR (126 MHz, C_6D_6, 297 K): $\delta = 31.4$ (s, $J_{C-117Sn} = 261.7$, $J_{C-119Sn} = 273.8$, $J_{C-117Sn} = 41.1$, $J_{C-119Sn} = 42.7$ Hz, *C*Me$_3$), 33.2 (s, $J_{C-117Sn} = 261.4$, $J_{C-119Sn} = 273.5$ Hz, *C*Me$_3$), 33.3 (s, CMe_3), 33.3 (s, CMe_3), 87.3 (s, *C*H, C_7H_6), 90.2 (s, $J_{C-117Sn} = 45.4$, $J_{C-119Sn} = 47.2$, $J_{C-117/119Sn} = 4.3$ Hz, *C*H, C_7H_6), 94.8 (s, $J_{C-117/119Sn} = 36.8$ Hz, *C*H, C_7H_6), 100.2 (s, $J_{C-117Sn} = 202.3$, $J_{C-119Sn} = 211.7$, $J_{C-117/119Sn} = 20.2$ Hz, C_{ipso}, C_7H_6), 100.7 (s, $J_{C-117/119Sn} = 25.8$ Hz, *C*H, C_5H_4), 106.9 (s, $J_{C-117/119Sn} = 29.8$ Hz, *C*H, C_5H_4), 112.7 ppm (s, $J_{C-117Sn} = 157.4$, $J_{C-119Sn} = 164.4$, $J_{C-117/119Sn} = 29.6$ Hz, C_{ipso}, C_5H_4); $^{119}Sn\{^1H\}$ NMR (187 MHz, C_6D_6, 297 K): $\delta = -28.4$ (s, $J_{Sn-117Sn} = 1144.4$, $J_{Sn-119Sn} = 1197.9$ Hz), −9.0 (s, $J_{Sn-117Sn} = 1144.4$, $J_{Sn-119Sn} = 1197.9$ Hz); λ_{max} (ε) = 681 nm (49 L mol^{-1} cm^{-1}); elemental analysis calcd (%) for $C_{28}H_{46}Sn_2Ti$ (667.95): C 50.35, H 6.94; found: C 50.37, H 6.86.

[Ti(η^5-C_5H_4)(η^7-C_7H_6)Sn(Mes)$_2$Pt(PEt$_3$)$_2$] (5): A 100 mL sealed Schlenk flask, charged with **3** (0.06 g, 0.11 mmol), $Pt(PEt_3)_3$ (0.06 g, 0.11 mmol), and toluene (10 mL), was heated under vacuum at 60 °C for 2 days, during which time the mixture turned green. Then the solution was vacuum dried and the residue was extracted with hexane and filtered through glass wool. Drying under high vacuum yielded a green solid. Recrystallization of the product from hexane at −30 °C resulted in the isolation of **4** as green crystals (0.07 g, 0.07 mmol, 66%). ^1H NMR (400 MHz, C_6D_6, 297 K): $\delta = 0.75$ (m, 9H; $P(CH_2CH_3)_3$), 0.88 (m, 9H; $P(CH_2CH_3)_3$), 0.99 (m, 6H; $P(CH_2CH_3)_3$), 1.23 (m, 6H; $P(CH_2CH_3)_3$), 2.23 (br, 6H; Me_{para}, Mes), 2.92 (s, $J_{H-117/119Sn} = 7.6$ Hz, 12H; Me_{ortho}, Mes), 5.03 (m, 4H; C_5H_4), 5.17 (m, 2H; C_7H_6), 5.80 (br m, 4H; C_7H_6), 6.89 ppm (s, $J_{H-117Sn} =$

11.5, $J_{H-119Sn}$ = 21 Hz, 4H; C*H*, Mes); $^{13}C\{^1H\}$ NMR (100 MHz, C_6D_6, 297 K): δ = 8.6 (s, $P(CH_2CH_3)_3$), 9.3 (s, $P(CH_2CH_3)_3$), 15.8 (d, J_{C-31P} = 23 Hz, $P(CH_2CH_3)_3$), 20.1 (d, J_{C-31P} = 24.1, $J_{C-195Pt}$ = 31.5 Hz, $P(CH_2CH_3)_3$), 21.6 (s, Me_{ortho}, Mes), 26.4 (s, $J_{H-117/119Sn}$ = 38 Hz, Me_{ortho}, Mes), 86.3 (s, $J_{C-195Pt}$ = 32 Hz, C_{ipso}, C_7H_6), 87.0 (s, C*H*, C_7H_6), 89.9 (s, C*H*, C_7H_6), 91.5 (s, C*H*, C_7H_6), 97.6 (s, C_{ipso}, C_5H_4), 101.7 (s, C*H*, C_5H_4), 103.0 ppm (s, C*H*, C_5H_4); $^{31}P\{^1H\}$ NMR (161 MHz, C_6D_6, 297 K): δ = 0.9 (d, J_{P-31P} = 16, $J_{P-195Pt}$ = 2104, $J_{P-117Sn}$ = 128, $J_{P-119Sn}$ = 160 Hz, $P(CH_2CH_3)_3$, *cis* to Sn), 9.9 ppm (d, J_{P-31P} = 16, $J_{P-195Pt}$ = 1978, $J_{P-117Sn}$ = 2222, $J_{P-119Sn}$ = 2327 Hz, $P(CH_2CH_3)_3$, *trans* to Sn); $^{119}Sn\{^1H\}$ NMR (149 MHz, C_6D_6, 297 K): δ = −152.5 ppm (dd, J_{Sn-31P} = 148 Hz, *cis* to P, J_{Sn-31P} = 2325 Hz, *trans* to P, $J_{Sn-195Pt}$ = 13302 Hz); elemental analysis calcd (%) for $C_{42}H_{62}P_2PtSnTi$ (990.55): C 50.93, H 6.31; found: C 52.23, H 6.46.

[Ti(η^5-C_5H_4Sn*t*Bu_2)(η^7-C_7H_6Sn*t*Bu_2)S] (6): Solid sulfur (0.07 g, 0.28 mmol) was added to a solution of [Ti(η^5-C_5H_4)(η^7-C_7H_6)Sn_2*t*Bu_4] (0.10 g, 0.14 mmol) in C_6D_6 (1.5 mL) and the reaction mixture was heated to 50 °C for 20 h. All volatiles were removed in vacuo and the residue was purified by chromatography over alumina activity grade V with hexane as eluent. [Ti(η^5-C_5H_4Sn*t*Bu_2)(η^7-C_7H_6Sn*t*Bu_2)S] (0.03 g, 0.05 mmol, 33 %) was obtained as a blue solid. ^1H NMR (500 MHz, C_6D_6, 297 K): δ = 1.37 (s, $J_{H-117Sn}$ = 75.2, $J_{H-119Sn}$ = 78.7 Hz, 18H; CMe_3), 1.54 (s, $J_{H-117Sn}$ = 73.4, $J_{H-119Sn}$ = 76.9 Hz, 18H; CMe_3), 5.23 (m, 4H; C_5H_4), 5.47–5.56 (m, 4H; C_7H_6), 5.76–5.88 ppm (m, 2H; C_7H_6); $^{13}C\{^1H\}$ NMR (126 MHz, C_6D_6, 297 K): δ = 31.1 (s, CMe_3), 31.6 (s, CMe_3), 33.4 (s, $J_{C-117Sn}$ = 399.8, $J_{C-119Sn}$ = 418.3 Hz, *C*Me$_3$), 35.1 (s, $J_{C-117Sn}$ = 377.7, $J_{C-119Sn}$ = 395.4 Hz, *C*Me$_3$), 87.5 (s, C*H*, C_7H_6), 88.5 (s, $J_{C-117/119Sn}$ = 61.5 Hz, C*H*, C_7H_6), 93.2 (s, $J_{C-117/119Sn}$ = 38.2 Hz, C*H*, C_7H_6), 96.7 (s, C_{ipso}, C_7H_6), 100.5 (s, $J_{C-117/119Sn}$ = 36.8 Hz, C*H*, C_5H_4), 104.6 (s, C_{ipso}, C_5H_4), 104.9 ppm (s, $J_{C-117/119Sn}$ = 38.4 Hz, C*H*, C_5H_4); $^{119}Sn\{^1H\}$ NMR (187 MHz, C_6D_6, 297 K): δ = 25.5 (s, $J_{Sn-117Sn}$ = 277.8, $J_{Sn-119Sn}$ = 291.5 Hz), 42.9 (s, $J_{Sn-117Sn}$ = 279.0, $J_{Sn-119Sn}$ = 292.1 Hz); elemental analysis calcd (%) for $C_{28}H_{46}SSn_2Ti$ (700.02): C 48.04, H 6.62, S 4.58; found: C 48.65, H 6.85, S 4.49.

[Ti(η^5-C_5H_4Sn*t*Bu_2)(η^7-C_7H_6Sn*t*Bu_2)Se] (7): A suspension of [Ti(η^5-C_5H_4)(η^7-C_7H_6)Sn_2*t*Bu_4] (0.02 g, 0.03 mmol) and red selenium (0.01 g, 0.13 mmol) in C_6D_6 (1.5 mL) was heated to 60 °C for 15 days. The solvent was removed under reduced pressure and the residue was purified by chromatography over alumina activity grade V with hexane as eluent. [Ti(η^5-C_5H_4Sn*t*Bu_2)(η^7-C_7H_6Sn*t*Bu_2)Se] (0.01 g, 0.01 mmol, 49 %) was isolated as a blue solid. ^1H NMR (500 MHz, C_6D_6, 297 K): δ = 1.37 (s, $J_{H-117Sn}$ = 73.7, $J_{H-119Sn}$ = 77.1 Hz, 18H; CMe_3), 1.53 (s, $J_{H-117Sn}$ = 75.4, $J_{H-119Sn}$ = 79.0 Hz, 18H; CMe_3), 5.23 (m, 4H; C_5H_4), 5.49 (m, 2H; C_7H_6), 5.53 (m, 2H; C_7H_6), 5.82 ppm (m, 2H; C_7H_6); $^{13}C\{^1H\}$ NMR (126 MHz, C_6D_6, 297 K): δ = 31.2 (s, CMe_3), 31.6 (s, CMe_3), 33.1 (s, *C*Me$_3$), 35.0 (s, *C*Me$_3$), 87.5 (C*H*, C_7H_6), 88.3 (s, $J_{C-117/119Sn}$ = 60.6 Hz, C*H*, C_7H_6), 93.4 (s, $J_{C-117/119Sn}$ = 38.9 Hz, C_7H_6), 96.6 (s, $J_{C-117/119Sn}$ = 8.6 Hz, C_{ipso}, C_7H_6), 100.5 (s, $J_{C-117/119Sn}$ = 36.5 Hz, *C*H, C_5H_4), 104.3 (s, $J_{C-117/119Sn}$ = 9.4 Hz, C_{ipso}, C_5H_4), 105.0 ppm (s, $J_{C-117/119Sn}$ = 38.1 Hz, *C*H, C_5H_4); $^{119}Sn\{^1H\}$ NMR (187 MHz, C_6D_6, 297 K): δ = 20.8 (s, $J_{Sn-77Se}$ = 1431.4, $J_{Sn-117Sn}$ = 251.7, $J_{Sn-119Sn}$ = 260.8 Hz), 47.7 (s, $J_{Sn-77Se}$ = 1364.2, $J_{Sn-117Sn}$ = 250.5, $J_{Sn-119Sn}$ = 259.6 Hz); elemental analysis calcd (%) for $C_{28}H_{46}SeSn_2Ti$ (746.91): C 45.03, H 6.21; found: C 45.08, H 6.30.

[Ti(η^5-C_5H_4)(η^7-C_7H_6)B_2(NMe_2)$_2$] (8): [Ti(η^5-C_5H_4Li)(η^7-C_7H_6Li)]·pmdta (0.32 g, 1.02 mmol) was suspended in diethyl ether (20 mL) and cooled to −78 °C for 10 min. A solution of $Cl_2B_2(NMe_2)_2$ (0.19 g, 1.02 mmol) in diethyl ether (10 mL) was added dropwise to this suspension with a dropping funnel. The reaction mixture was slowly allowed to warm to room temperature and stirring was continued overnight. The resultant blue solution was filtered though celite and dried under high vacuum. [Ti(η^5-C_5H_4)(η^7-C_7H_6)$B_2(NMe_2)_2$] was obtained as a blue crystalline solid in pure form by recrystallization from diethyl ether solution at −30 °C (0.21 g, 0.67 mmol, 67 %). ^1H NMR (500 MHz, C_6D_6, 297 K): δ = 2.77 (s, 3H; NMe_2), 2.80 (s, 3H; NMe_2), 2.81 (s, 3H; NMe_2), 3.13 (s, 3H; NMe_2), 5.04 (m, 2H; C_5H_4), 5.26 (m, 2H; C_7H_6), 5.37 (m, 2H; C_5H_4), 5.85 ppm (m, 4H; C_7H_6); $^{11}B\{^1H\}$ NMR (160 MHz, C_6D_6, 297 K): δ = 42.0 (s), 45.5 ppm (s); $^{13}C\{^1H\}$ NMR (126 MHz, C_6D_6, 297 K): δ = 40.2 (s, NMe_2), 40.6 (s, NMe_2), 43.9 (s, NMe_2), 44.1 (s, NMe_2), 89.3 (s, *C*H, C_7H_6), 89.8 (s, *C*H, C_7H_6), 93.0 (s, *C*H, C_7H_6), 99.6 (s, *C*H, C_5H_4), 103.0 ppm (s, *C*H, C_5H_4); λ_{max} (ε) = 675 nm (77 L mol^{-1} cm^{-1}); elemental analysis calcd (%) for $C_{16}H_{22}B_2N_2Ti$ (311.85): C 61.62, H 7.11, N 8.98; found: C 61.31, H 7.00, N 8.88.

[Ti(η^5-$C_5H_4BNMe_2$)(η^7-$C_7H_6BNMe_2$)Pt(PEt_3)$_2$] (9): A 100 mL sealed Schlenk flask, charged with [Ti(η^5-C_5H_4)(η^7-C_7H_6)$B_2(NMe_2)_2$] (0.05 g, 0.14 mmol), [Pt(PEt_3)$_3$] (0.08 g, 0.14 mmol), and toluene (10 mL), was heated under vacuum at 60 °C for 4 days. All volatiles were removed in vacuo, and the residue was taken up in hexane and filtered through a short pad of celite. After removal of the solvent under reduced pressure, the remaining solid was redissolved in diethyl ether. Crystallization at −30 °C resulted in the isolation of [Ti(η^5-$C_5H_4BNMe_2$)(η^7-$C_7H_6BNMe_2$)Pt(PEt_3)$_2$] as blue crystals (0.08 g, 0.11 mmol, 79 %). ^1H NMR (500 MHz, C_6D_6, 297 K): δ = 0.92 (dt, J_{H-31P} = 13.9, J_{H-H} = 7.1 Hz, 9H; $P(CH_2CH_3)_3$), 1.09 (dt, J_{H-31P} = 14.1, J_{H-H} = 7.1 Hz, 9H; $P(CH_2CH_3)_3$), 1.58 (m, 6H; $P(CH_2CH_3)_3$), 1.70–1.80 (m, 6H; $P(CH_2CH_3)_3$), 3.02 (s, 3H; NMe_2), 3.22 (s, 3H; NMe_2), 3.26 (s, 3H; NMe_2), 3.33 (s, 3H; NMe_2), 5.19 (m, 1H; C_5H_4), 5.29 (m, 1H; C_5H_4), 5.63 (m, 1H; C_5H_4), 5.71 (m, 2H; C_7H_6), 5.81 (m, 2H; C_7H_6), 5.95 (m, 1H; C_7H_6), 6.12 (m, 1H; C_5H_4), 6.23 ppm (m, 1H; C_7H_6); $^{11}B\{^1H\}$ NMR (160 MHz, C_6D_6, 297 K): δ = 57.6 (br s), 62.7 ppm (br s); $^{13}C\{^1H\}$ NMR (126 MHz, C_6D_6, 297 K): δ = 8.6 (s, $J_{C-195Pt}$ = 15.0 Hz, $P(CH_2CH_3)_3$), 8.9 (s, $J_{C-195Pt}$ = 16.9 Hz, $P(CH_2CH_3)_3$), 20.0 (m, $P(CH_2CH_3)_3$) , 20.9 (m, $P(CH_2CH_3)_3$), 42.0 (d, J_{C-31P} = 3.2, $J_{C-195Pt}$ = 32.2 Hz, NMe_2), 42.5 (d, J_{C-31P} = 4.0, $J_{C-195Pt}$ = 36.0 Hz, NMe_2), 48.0 (d, J_{C-31P} = 4.0, $J_{C-195Pt}$ = 101.0 Hz, NMe_2), 49.5 (d, J_{C-31P} = 4.0, $J_{C-195Pt}$ = 101.6 Hz, NMe_2), 86.2 (s, *C*H, C_7H_6), 87.0 (s, $J_{C-195Pt}$ = 10.5 Hz, *C*H, C_7H_6), 87.9 (s, *C*H, C_7H_6), 89.7 (s, *C*H, C_7H_6), 90.6 (s, *C*H, C_7H_6), 94.2 (s, $J_{C-195Pt}$ = 29.6 Hz, *C*H, C_7H_6), 98.1 (s, $J_{C-195Pt}$ = 10.8 Hz, *C*H, C_4H_5), 98.9 (s, *C*H, C_5H_4), 103.2 (d, J_{C-31P} = 2.6, $J_{C-195Pt}$ = 19.1 Hz, *C*H, C_5H_4), 108.6 ppm (s, $J_{C-195Pt}$ = 33.0 Hz, *C*H, C_5H_4); $^{31}P\{^1H\}$ NMR (202 MHz, C_6D_6, 297 K): δ = 10.0 (br s, $J_{P-195Pt}$ = 1062.6 Hz), 10.7 (br s, $J_{P-195Pt}$ = 1171.0 Hz); elemental analysis calcd (%) for $C_{28}H_{52}B_2N_2P_2PtTi$ (743.24): C 45.25, H 7.05, N 3.77; found: C 45.32, H 7.06, N 3.72.

[Ti(η^5-C_5H_4)(η^7-C_7H_6)Si_2Me_4] (10): A slurry of [Ti(η^5-C_5H_4Li)(η^7-C_7H_6Li)]·pmdta (0.50 g, 1.29 mmol) in hexane (15 mL) was cooled to −78 °C and a solution of $Cl_2Si_2Me_4$ (0.29 g, 1.55 mmol) in hexane (5 mL) was added over a period of 2 h. After complete addition, the reaction mixture was stirred for another 2 h at −78 °C and subsequently allowed to reach ambient temperature. Stirring was continued for another 16 h at RT, during which time a white solid precipitated. The suspension was filtered and all volatiles were removed in vacuo. The product was purified by chromatography over alumina activity grade V with hexane as eluent, yielding [Ti(η^5-C_5H_4)(η^7-C_7H_6)Si_2Me_4] (0.26 g, 0.82 mmol, 63 %) as a blue solid. ^1H NMR (500 MHz, C_6D_6, 297 K): δ = 0.28 (s, 6H; SiMe_2), 0.50 (s, 6H; SiMe_2), 5.03 (m, 2H; C_5H_4), 5.40 (m, 2H; C_5H_4), 5.58–5.62 (m, 2H; C_7H_6), 5.72–5.78 ppm (m, 4H; C_7H_6); $^{13}C\{^1H\}$ NMR (126 MHz, C_6D_6, 297 K): δ = −2.4 (s, SiMe_2), −2.2 (s, SiMe_2), 88.3 (s, *C*H, C_7H_6), 90.4 (s, *C*H, C_7H_6), 92.0 (s, *C*H, C_7H_6), 94.4 (s, C_{ipso}, C_7H_6), 100.5 (s, *C*H, C_5H_4), 104.8 (s, *C*H, C_5H_4), 113.0 ppm (s, C_{ipso}, C_5H_4); $^{29}Si\{^1H\}$ NMR (99 MHz, C_6D_6, 297 K): δ = −19.8 (s), −12.1 ppm (s); λ_{max} (ε) = 678 nm (45 L mol^{-1} cm^{-1}); elemental analysis calcd (%) for $C_{16}H_{22}Si_2Ti$ (318.38): C 60.36, H 6.96; found: C 60.37, H 6.94.

[Ti(η^5-$C_5H_4SiMe_2$)(η^7-$C_7H_6SiMe_2$)CH_2] (11): A slurry of [Ti(η^5-C_5H_4Li)(η^7-C_7H_6Li)]·pmdta (0.50 g, 1.29 mmol) in hexane (10 mL) was cooled to −78 °C and treated dropwise with a solution of $(ClSiMe_2)_2CH_2$ (0.28 g, 1.41 mmol) in hexane (10 mL). After complete addition the reaction mixture was allowed to reach ambient temperature and was stirred overnight. The suspension was filtered, the solvent was removed under reduced pressure, and the product was purified by chromatography over alumina activity grade V with hexane as eluent. [Ti(η^5-$C_5H_4SiMe_2$)(η^7-$C_7H_6SiMe_2$)CH_2] (0.17 g, 0.50 mmol, 40 %) was obtained as a blue solid. ^1H NMR (500 MHz, C_6D_6, 297 K): δ = 0.03 (s, 2H; CH_2), 0.16 (s, 6H; SiMe_2), 0.45 (s, 6H; SiMe_2), 5.02 (m, 2H; C_5H_4), 5.10 (m, 2H; C_5H_4), 5.53 ppm (m, 6H; C_7H_6); $^{13}C\{^1H\}$ NMR (126 MHz, C_6D_6, 297 K): δ = 0.5 (s, SiMe_2), 0.7 (s, SiMe_2), 8.8 (s, CH_2), 86.6 (s, *C*H, C_7H_6), 90.2 (s, *C*H, C_7H_6), 90.8 (s, *C*H, C_7H_6), 94.9 (s, C_{ipso}, C_7H_6), 100.1 (s, *C*H, C_5H_4), 103.4 (s, *C*H, C_5H_4), 110.3 ppm (s, C_{ipso}, C_5H_4); $^{29}Si\{^1H\}$ NMR (99 MHz, C_6D_6, 297 K): δ = −8.3 (s), 1.5 ppm (s); λ_{max} (ε) = 666 nm (38 L mol^{-1} cm^{-1}); elemental analysis calcd (%) for $C_{17}H_{24}Si_2Ti$ (332.41): C 61.42, H 7.28;. found: C 61.38, H 7.63.

Single-crystal X-ray structure determination: The crystal data were collected on Bruker X8 APEX-2 (**6**, **8**, **11**), Bruker D8 APEX-1 (**4**), Oxford Xcalibur Eos (**3**, **9**), and Oxford Xcalibur Nova (**5**, **10**) diffractometers. Structures **5** and **10** were measured with $Cu_{K\alpha}$ radiation, all others with $Mo_{K\alpha}$ radiation. Structures were refined anisotropically with the program SHELXL-97.[50] Hydrogen atoms were assigned idealized positions and then refined by using a riding model or rigid methyl groups.

CCDC-778694 (**3**), 778695 (**4**), 778696 (**5**), 778697 (**6**), 778698 (**8**), 778699 (**9**), 778700 (**10**), and 778701 (**11**) contain the supplementary crystallographic data for this paper. These data can be obtained free of charge from The Cambridge Crystallographic Data Centre via www.ccdc.cam.ac.uk/data_request/cif.

Crystal data for ***3***: $C_{78}H_{110}Br_2Li_2N_6Sn_2Ti_2$; $M_r=1638.60$; blue prism; $0.11\times0.15\times0.17\ mm^3$; monoclinic; space group $P2_1/n$; $a=11.8012(2)$, $b=11.3998(2)$, $c=29.4621(6)$ Å; $\beta=98.842(2)°$; $V=3916.47(12)$ Å^3; $Z=2$; $\rho_{calcd}=1.389\ g\,cm^{-3}$; $\mu=1.891\ mm^{-1}$; $F(000)=1680$; $T=100(2)$ K; $R_1=0.0398$, $wR_2=0.1033$; 8957 independent reflections [$2\theta\leq54.9°$] and 426 parameters.[32]

Crystal data for ***4***: $C_{28}H_{46}Sn_2Ti$; $M_r=667.93$; blue plate; $0.08\times0.20\times0.40\ mm^3$; monoclinic; space group $P2_1/c$; $a=17.9732(10)$, $b=10.7719(6)$, $c=32.4171(19)$ Å; $\beta=100.0760(10)°$; $V=6179.3(6)$ Å^3; $Z=8$; $\rho_{calcd}=1.436\ g\,cm^{-3}$; $\mu=1.868\ mm^{-1}$; $F(000)=2688$; $T=174(2)$ K; $R_1=0.0469$, $wR_2=0.0935$; 12253 independent reflections [$2\theta\leq52.2°$] and 591 parameters.

Crystal data for ***5***: $C_{42}H_{62}P_2SnTiPt$; $M_r=990.54$; blue prism; $0.03\times0.04\times0.04\ mm^3$; monoclinic; space group $P2_1/n$; $a=18.3308(2)$, $b=19.6944(2)$, $c=22.5532(3)$ Å; $\beta=90.3058(9)°$; $V=8141.93(14)$ Å^3; $Z=8$; $\rho_{calcd}=1.616\ g\,cm^{-3}$; $\mu=13.705\ mm^{-1}$; $F(000)=3952$; $T=100(2)$ K; $R_1=0.0318$, $wR_2=0.0843$; 16905 independent reflections [$2\theta\leq151.9°$] and 871 parameters.

Crystal data for ***6***: $C_{28}H_{46}SSn_2Ti$; $M_r=699.99$; blue needle; $0.36\times0.16\times0.06\ mm^3$; trigonal; space group $P\bar{3}$; $a=32.6831(14)$, $b=32.6831(14)$, $c=15.2394(8)$ Å; $V=14097.6(11)$ Å^3; $Z=18$; $\rho_{calcd}=1.484\ g\,cm^{-3}$; $\mu=1.910\ mm^{-1}$; $F(000)=6336$; $T=100(2)$ K; $R_1=0.0442$, $wR_2=0.1107$; 18951 independent reflections [$2\theta\leq52.74°$] and 901 parameters.

Crystal data for ***8***: $C_{16}H_{22}B_2N_2Ti$; $M_r=311.88$; blue block; $0.18\times0.08\times0.06\ mm^3$; orthorhombic; space group $P2_12_12_1$; $a=10.811(3)$, $b=11.790(3)$, $c=12.190(4)$ Å; $V=1553.6(8)$ Å^3; $Z=4$; $\rho_{calcd}=1.333\ g\,cm^{-3}$; $\mu=0.543\ mm^{-1}$; $F(000)=656$; $T=173(2)$ K; $R_1=0.0282$, $wR_2=0.0660$; 3816 independent reflections [$2\theta\leq56.56°$] and 194 parameters.

Crystal data for ***9***: $C_{31}H_{59}B_2N_2P_2TiPt$; $M_r=786.35$; blue prism; $0.27\times0.29\times0.30\ mm^3$; monoclinic; space group $P2_1/n$; $a=11.6272(2)$, $b=15.7831(2)$, $c=19.2703(4)$ Å; $\beta=102.560(2)°$; $V=3451.73(10)$ Å^3; $Z=4$; $\rho_{calcd}=1.513\ g\,cm^{-3}$; $\mu=4.395\ mm^{-1}$; $F(000)=1596$; $T=100(2)$ K; $R_1=0.0154$, $wR_2=0.0337$; 9256 independent reflections [$2\theta\leq58.2°$] and 363 parameters. The compound crystallizes with half a molecule of well-ordered hexane in the asymmetric unit.

Crystal data for ***10***: $C_{16}H_{22}Si_2Ti$; $M_r=318.42$; blue plate; $0.04\times0.04\times0.07\ mm^3$; orthorhombic; space group $Pbca$; $a=8.1803(4)$, $b=17.7967(10)$, $c=22.0823(10)$ Å; $V=3214.8(3)$ Å^3; $Z=8$; $\rho_{calcd}=1.316\ g\,cm^{-3}$; $\mu=5.796\ mm^{-1}$; $F(000)=1344$; $T=100(2)$ K; $R_1=0.0422$, $wR_2=0.0952$; 3182 independent reflections [$2\theta\leq146.8°$] and 176 parameters.

Crystal data for ***11***: $C_{17}H_{24}Si_2Ti$; $M_r=332.44$; blue block; $0.11\times0.096\times0.069\ mm^3$; tetragonal; space group $I4_1/a$; $a=26.6752(16)$, $b=26.6752(16)$, $c=9.5920(6)$ Å; $V=6825.3(7)$ Å^3; $Z=16$; $\rho_{calcd}=1.294\ g\,cm^{-3}$; $\mu=0.631\ mm^{-1}$; $F(000)=2816$; $T=100(2)$ K; $R_1=0.0578$, $wR_2=0.1328$; 3368 independent reflections [$2\theta\leq52.12°$] and 246 parameters.

Acknowledgements

This work was supported by the Deutsche Forschungsgemeinschaft (DFG) and the Fonds der Chemischen Industrie (FCI).

[1] A. G. Osborne, R. H. Whiteley, *J. Organomet. Chem.* **1975**, *101*, C27.
[2] a) A. S. Abd-El-Aziz, I. Manners (Eds.), *Frontiers in Transition Metal Containing Polymers*; John Wiley and Sons, Inc., Hoboken, New Jersey, **2007**; b) D. E. Herbert, U. F. J. Mayer, I. Manners, *Angew. Chem.* **2007**, *119*, 5152; *Angew. Chem. Int. Ed.* **2007**, *46*, 5060; c) W. Finckh, B. Z. Tang, D. A. Foucher, D. B. Zamble, R. Ziembinski, A. Lough, I. Manners, *Organometallics* **1993**, *12*, 823; d) V. Bellas, M. Rehahn, *Angew. Chem.* **2007**, *119*, 5174; *Angew. Chem. Int. Ed.* **2007**, *46*, 5082; e) C. Cui, J. Heilmann-Brohl, A. Sanchez Perucha, M. D. Thomson, H. G. Roskos, M. Wagner, F. Jaekle, *Macromolecules* **2010**, *43*, 5256; f) M. Scheibitz, H. Li, J. Schnorr, A. Sanchez Perucha, M. Bolte, H. W. Lerner, F. Jaekle, M. Wagner, *J. Am. Chem. Soc.* **2009**, *131*, 16319; g) J. B. Heilmann, Y. Qin, F. Jaekle, H. W. Lerner, M. Wagner, *Inorg. Chim. Acta* **2006**, *359*, 4802; h) J. B. Heilmann, M. Scheibitz, Y. Qin, A. Sundararaman, F. Jaekle, T. Kretz, M. Bolte, H. W. Lerner, M. C. Holthausen, M. Wagner, *Angew. Chem.* **2006**, *118*, 934; *Angew. Chem. Int. Ed.* **2006**, *45*, 920.
[3] a) A. Berenbaum, H. Braunschweig, R. Dirk, U. Englert, J. C. Green, F. Jäkle, A. J. Lough, I. Manners, *J. Am. Chem. Soc.* **2000**, *122*, 5765; b) J. A. Schachner, C. L. Lund, J. Wilson Quail, J. Müller, *Organometallics* **2005**, *24*, 785; c) J. A. Schachner, C. L. Lund, J. Wilson Quail, J. Müller, *Organometallics* **2005**, *24*, 4483.
[4] a) A. G. Osborne, R. H. Whiteley, R. E. Meads, *J. Organomet. Chem.* **1980**, *193*, 345; b) D. A. Foucher, M. Edwards, R. A. Burrow, A. J. Lough, I. Manners, *Organometallics* **1994**, *13*, 4959; c) R. Rulkens, A. J. Lough, I. Manners, *Angew. Chem.* **1996**, *108*, 1929; *Angew. Chem. Int. Ed. Engl.* **1996**, *35*, 1805; d) F. Jäkle, R. Rulkens, G. Zech, D. A. Foucher, A. J. Lough, I. Manners, *Chem. Eur. J.* **1998**, *4*, 2117.
[5] a) H. Stoeckli-Evans, A. G. Osborne, R. H. Whiteley, *J. Organomet. Chem.* **1980**, *194*, 91; b) D. Seyferth, H. P. Withers, *Organometallics* **1982**, *1*, 1275; c) I. R. Butler, W. R. Cullen, F. W. B. Einstein, S. J. Rettig, A. J. Willis, *Organometallics* **1983**, *2*, 128.
[6] a) J. K. Pudelski, D. P. Gates, R. Rulkens, A. J. Lough, I. Manners, *Angew. Chem.* **1995**, *107*, 1633; *Angew. Chem. Int. Ed. Engl.* **1995**, *34*, 1506; b) R. Rulkens, D. P. Gates, D. Balaishis, J. K. Pudelski, D. F. McIntosh, A. J. Lough, I. Manners, *J. Am. Chem. Soc.* **1997**, *119*, 10976.
[7] R. Broussier, A. Da Rold, B. Gautheron, Y. Dromzee, Y. Jeannin, *Inorg. Chem.* **1990**, *29*, 1817.
[8] G. R. Whittell, B. M. Partridge, O. C. Presly, C. J. Adams, I. Manners, *Angew. Chem.* **2008**, *120*, 4426; *Angew. Chem. Int. Ed.* **2008**, *47*, 4354.
[9] a) J. M. Nelson, A. J. Lough, I. Manners, *Angew. Chem.* **1994**, *106*, 1019; *Angew. Chem. Int. Ed. Engl.* **1994**, *33*, 989; b) U. Vogel, A. J. Lough, I. Manners, *Angew. Chem.* **2004**, *116*, 3383; *Angew. Chem. Int. Ed.* **2004**, *43*, 3321.
[10] a) M. J. Drewitt, S. Barlow, D. O'Hare, J. M. Nelson, P. Nguyen, I. Manners, *Chem. Commun.* **1996**, 2153; b) S. Fox, J. P. Dunne, M. Tacke, D. Schmitz, R. Dronskowski, *Eur. J. Inorg. Chem.* **2002**, 3039; c) H. Braunschweig, F. Breher, M. Kaupp, M. Gross, T. Kupfer, D. Nied, K. Radacki, S. Schinzel, *Organometallics* **2008**, *27*, 6427; d) U. F. J. Mayer, J. B. Gilroy, D. O'Hare, I. Manners, *J. Am. Chem. Soc.* **2009**, *131*, 10382.
[11] H. Braunschweig, M. Gross, K. Radacki, *Organometallics* **2007**, *26*, 6688.
[12] a) H. Braunschweig, C. J. Adams, T. Kupfer, I. Manners, R. Richardson, G. R. Whittell, *Angew. Chem.* **2008**, *120*, 3886; *Angew. Chem. Int. Ed.* **2008**, *47*, 3826; b) H. Braunschweig, M. Kaupp, C. J. Adams, T. Kupfer, K. Radacki, S. Schinzel, *J. Am. Chem. Soc.* **2008**, *130*, 11376; c) A. Berenbaum, I. Manners, *Dalton Trans.* **2004**, 2057; d) C. Elschenbroich, E. Schmidt, R. Gondrum, B. Metz, O. Burghaus, W. Massa, S. Wocadlo, *Organometallics* **1997**, *16*, 4589; e) C. Elschenbroich, A. Bretschneider-Hurley, J. Hurley, A. Behrendt, W. Massa, S. Wocadlo, E. Reijerse, *Inorg. Chem.* **1995**, *34*, 743; f) C. Elschenbroich, A. Bretschneider-Hurley, J. Hurley, W. Massa, S. Wocadlo, J. Pebler, *Inorg. Chem.* **1993**, *32*, 5421.

[13] a) C. L. Lund, J. A. Schachner, J. Wilson Quail, J. Müller, *Organometallics* **2006**, *25*, 5817; b) C. Elschenbroich, E. Schmidt, B. Metz, K. Harms, *Organometallics* **1995**, *14*, 4043.
[14] a) H. Braunschweig, T. Kupfer, *Organometallics* **2007**, *26*, 4634; b) H. Braunschweig, M. Homberger, C. Hu, X. Zheng, E. Gullo, G. Clentsmith, M. Lutz, *Organometallics* **2004**, *23*, 1968; c) C. Elschenbroich, J. Hurley, B. Metz, W. Massa, G. Baum, *Organometallics* **1990**, *9*, 889; d) K. C. Hultzsch, J. M. Nelson, A. J. Lough, I. Manners, *Organometallics* **1995**, *14*, 5496.
[15] a) C. L. Lund, J. A. Schachner, J. W. Quail, J. Müller, *J. Am. Chem. Soc.* **2007**, *129*, 9313; b) H. Braunschweig, N. Buggisch, U. Englert, M. Homberger, T. Kupfer, D. Leusser, M. Lutz, K. Radacki, *J. Am. Chem. Soc.* **2007**, *129*, 4840; c) C. L. Lund, J. A. Schachner, I. J. Burgess, J. W. Quail, G. Schatte, J. Müller, *Inorg. Chem.* **2008**, *47*, 5992; d) C. L. Lund, B. Bagh, J. W. Quail, J. Müller, *Organometallics* **2010**, *29*, 1977.
[16] C. Elschenbroich, F. Paganelli, M. Nowotny, B. Neumüller, O. Burghaus, *Z. Anorg. Allg. Chem.* **2004**, *630*, 1599.
[17] H. Braunschweig, T. Kupfer, *Acc. Chem. Res.* **2010**, *43*, 455.
[18] M. Tamm, *Chem. Commun.* **2008**, 3089.
[19] M. L. H. Green, D. G. K. Ng, *Chem. Rev.* **1995**, *95*, 439.
[20] a) M. Tamm, A. Kunst, T. Bannenberg, E. Herdtweck, P. Sirsch, C. J. Elsevier, J. M. Ernsting, *Angew. Chem.* **2004**, *116*, 5646; *Angew. Chem. Int. Ed.* **2004**, *43*, 5530; b) M. Tamm, A. Kunst, E. Herdtweck, *Chem. Commun.* **2005**, 1729; c) M. Tamm, A. Kunst, T. Bannenberg, S. Randoll, P. G. Jones, *Organometallics* **2007**, *26*, 417.
[21] a) S. Büschel, A.-K. Jungton, T. Bannenberg, S. Randoll, C. G. Hrib, P. G. Jones, M. Tamm, *Chem. Eur. J.* **2009**, *15*, 2176; b) S. Büschel, C.-G. Daniliuc, P. G. Jones, M. Tamm, *Organometallics* **2010**, *29*, 671; c) S. Büschel, T. Bannenberg, C. G. Hrib, A. Glöckner, P. G. Jones, M. Tamm, *J. Organomet. Chem.* **2009**, *694*, 1244.
[22] a) C. Elschenbroich, J. Plackmeyer, M. Nowotny, A. Behrendt, K. Harms, J. Pebler, O. Burghaus, *Chem. Eur. J.* **2005**, *11*, 7427; b) C. Elschenbroich, J. Plackmeyer, M. Nowotny, K. Harms, J. Pebler, O. Burghaus, *Inorg. Chem.* **2005**, *44*, 955; c) C. Elschenbroich, M. Wolf, J. Pebler, K. Harms, *Organometallics* **2004**, *23*, 454; d) C. Elschenbroich, J. Plackmeyer, K. Harms, O. Burghaus, J. Pebler, *Organometallics* **2003**, *22*, 3367; e) C. Elschenbroich, M. Wolf, O. Schiemann, K. Harms, O. Burghaus, J. Pebler, *Organometallics* **2002**, *21*, 5810; f) C. Elschenbroich, F. Lu, K. Harms, *Organometallics* **2002**, *21*, 5152; g) C. Elschenbroich, O. Schiemann, O. Burghaus, K. Harms, J. Pebler, *Organometallics* **1999**, *18*, 3273; h) C. Elschenbroich, M. Wolf, O. Burghaus, K. Harms, J. Pebler, *Eur. J. Inorg. Chem.* **1999**, 2173.
[23] H. Braunschweig, M. Lutz, K. Radacki, A. Schaumlöffel, F. Seeler, C. Unkelbach, *Organometallics* **2006**, *25*, 4433.
[24] a) H. Braunschweig, M. Lutz, K. Radacki, *Angew. Chem.* **2005**, *117*, 5792; *Angew. Chem. Int. Ed.* **2005**, *44*, 5647; b) A. Bartole-Scott, H. Braunschweig, T. Kupfer, M. Lutz, I. Manners, T. Nguyen, K. Radacki, F. Seeler, *Chem. Eur. J.* **2006**, *12*, 1266; c) H. Braunschweig, T. Kupfer, M. Lutz, K. Radacki, *J. Am. Chem. Soc.* **2007**, *129*, 8893.
[25] S. K. Mohapatra, S. Büschel, C. Daniliuc, P. G. Jones, M. Tamm, *J. Am. Chem. Soc.* **2009**, *131*, 17014.
[26] H. Braunschweig, T. Kupfer, K. Radacki, *Angew. Chem.* **2007**, *119*, 1655; *Angew. Chem. Int. Ed.* **2007**, *46*, 1630.
[27] P. Chadha, J. L. Dutton, M. J. Sgro, P. J. Ragogna, *Organometallics* **2007**, *26*, 6063.
[28] a) B. Demerseman, P. H. Dixneuf, J. Douglade, R. Mercier, *Inorg. Chem.* **1982**, *21*, 3942; b) H. O. Van Oven, H. J. Liefde Meijer, *J. Organomet. Chem.* **1970**, *23*, 159; c) B. Demerseman, G. Bouquet, M. Bigorgne, *J. Organomet. Chem.* **1975**, *101*, C24.
[29] G. Fraenkel, R. E. Carter, A. McLachlan, J. H. Richards, *J. Am. Chem. Soc.* **1960**, *82*, 5846.
[30] a) H. Braunschweig, T. Kupfer, M. Lutz, K. Radacki, F. Seeler, R. Sigritz, *Angew. Chem.* **2006**, *118*, 8217; *Angew. Chem. Int. Ed.* **2006**, *45*, 8048; b) H. Braunschweig, T. Kupfer, *J. Am. Chem. Soc.* **2008**, *130*, 4242.
[31] P. Brown, M. F. Mahon, K. C. Molloy, *J. Organomet. Chem.* **1992**, *435*, 265.
[32] The asymmetric unit contains one molecule of **3** and one half of the centrosymmetric bromide-bridged dimer $[LiBr(pmdta)]_2$; the structural parameters are very similar to those published for an authentic sample of $[LiBr(pmdta)]_2$, see: S. R. Hall, C. L. Raston, B. W. Skelton, A. H. White, *Inorg. Chem.* **1983**, *22*, 4070.
[33] K. A. Lyssenko, M. Y. Antipin, S. Y. Ketkov, *Russ. Bull. Int. Ed.* **2001**, *50*, 130.
[34] W. Zheng, D. W. Stephan, *Inorg. Chem.* **1988**, *27*, 2386.
[35] J. M. Allen, J. E. Ellis, *J. Organomet. Chem.* **2008**, *693*, 1536.
[36] a) M. Herberhold, U. Steffl, W. Milius, B. Wrackmeyer, *Angew. Chem.* **1997**, *109*, 1545; *Angew. Chem. Int. Ed. Engl.* **1997**, *36*, 1508; b) M. Herberhold, U. Steffl, W. Milius, B. Wrackmeyer, *Chem. Eur. J.* **1998**, *4*, 1027; c) M. Herberhold, U. Steffl, B. Wrackmeyer, *J. Organomet. Chem.* **1999**, *577*, 76.
[37] H. Bera, H. Braunschweig, R. Doerfler, K. Hammond, A. Oechsner, K. Radacki, K. Uttinger, *Chem. Eur. J.* **2009**, *15*, 12092.
[38] M. Herberhold, U. Steffl, W. Milius, B. Wrackmeyer, *Angew. Chem.* **1996**, *108*, 1927; *Angew. Chem. Int. Ed. Engl.* **1996**, *35*, 1803.
[39] L. Kollár, S. Gladiali, M. J. Tenorio, W. Weissensteiner, *J. Cluster Sci.* **1998**, *9*, 321.
[40] M. Herberhold, U. Steffl, W. Milius, B. Wrackmeyer, *J. Organomet. Chem.* **1997**, *533*, 109.
[41] J. D. Zeinstra, J. L. De Boer, *J. Organomet. Chem.* **1973**, *54*, 207.
[42] a) T. Ishiyama, N. Miyaura, *J. Organomet. Chem.* **2000**, *611*, 392; b) H. Braunschweig, C. Kollann, D. Rais, *Angew. Chem.* **2006**, *118*, 5380; *Angew. Chem. Int. Ed.* **2006**, *45*, 5254; c) A. Kerr, T. B. Marder, N. C. Norman, A. G. Orpen, M. J. Quayle, C. R. Rice, P. L. Timms, G. R. Whittell, *Chem. Commun.* **1998**, 319; d) W. Clegg, F. J. Lawlor, G. Lesley, T. B. Marder, N. C. Norman, A. G. Orpen, M. J. Quayle, C. R. Rice, A. J. Scott, F. E. S. Souza, *J. Organomet. Chem.* **1998**, *550*, 183; e) C. N. Iverson, M. R. Smith III, *Organometallics* **1996**, *15*, 5155; f) G. Lesley, P. Nguyen, N. J. Taylor, T. B. Marder, A. J. Scott, W. Clegg, N. C. Norman, *Organometallics* **1996**, *15*, 5137; g) T. Ishiyama, N. Matsuda, M. Murata, F. Ozawa, A. Suzuki, N. Miyaura, *Organometallics* **1996**, *15*, 713; h) C. N. Iverson, M. R. Smith III, *J. Am. Chem. Soc.* **1995**, *117*, 4403; i) T. Ishiyama, N. Matsuda, N. Miyaura, A. Suzuki, *J. Am. Chem. Soc.* **1993**, *115*, 11018.
[43] M. D. Rausch, M. Ogasa, R. D. Rogers, A. N. Rollins, *Organometallics* **1991**, *10*, 2084.
[44] T. K. Panda, M. T. Gamer, P. W. Roesky, *Organometallics* **2003**, *22*, 877.
[45] L. E. Manxzer, *Inorg. Synth.* **1982**, *21*, 135.
[46] U. Englich, U. Hermann, I. Prass, T. Schollmeier, K. Ruhlandt-Senge, F. Ulig, *J. Organomet. Chem.* **2002**, *646*, 271.
[47] W. Einholz, W. Gollinger, W. Haubold, *Z. Naturforsch.* **1990**, *B45*, 25.
[48] a) H. Nöth, H. Schick, W. Meister, *J. Organomet. Chem.* **1964**, *1*, 401; <*lit* b>J. T. Patton, S. G. Feng, *Organometallics* **2001**, *20*, 3399.
[49] T. Yoshida, T. Matsuda, S. Otsuka, *Inorg. Synth.* **1990**, *28*, 119.
[50] G. Sheldrick, *Acta Crystallogr. Sect. A* **2008**, *64*, 112.

Received: May 28, 2010
Published online: August 27, 2010

